JNCC/Cefas Partnership Report Series

Report No. 24

Offshore seabed survey of Wight-Barfleur Reef SAC

Barrio Froján, C., Diesing, M. & Rance, J.

September 2021

ISSN 2051-6711

Offshore seabed survey of Wight-Barfleur Reef SAC

Christopher Barrio Froján, Markus Diesing & Julia Rance

September 2021

ISSN 2051-6711

For further information please contact:
Joint Nature Conservation Committee
Monkstone House
City Road
Peterborough PE1 1JY
www.jncc.gov.uk

This report should be cited as:
Barrio Froján, C., Diesing, M. & Rance, J. (2021). Offshore seabed survey of Wight-Barfleur Reef SAC. *JNCC/Cefas Partnership Report Series No. 24*. JNCC, Peterborough. ISSN 2051-6711.

This report is compliant with the JNCC **Evidence Quality Assurance Policy** https://jncc.gov.uk/about-jncc/corporate-information/evidence-quality-assurance/. This report was reviewed by Cefas and JNCC, with comments and input from an external contractor who was employed by JNCC for the purposes of this project.

Executive Summary

This report describes the findings of a dedicated survey by JNCC in partnership with Cefas to Wight Barfleur Reef Special Area of Conservation. Located in the central English Channel, Wight Barfleur Reef is characterised by a series of well-defined exposed bedrock ridges, up to 5m high, together with areas of flat, smooth mudstone and sandstone with overlying coarse sediment (gravels, cobbles and boulders), which in places forms stony reef, which has been designated to protect the EU Habitats Directive (1992) Annex I habitat feature “Reefs”.

The dedicated multidisciplinary survey (survey code CEND 03/13) was conducted in March 2013 aboard the RV Cefas Endeavour with the principal aim of collecting information to better delineate the extent of Annex I reef (both bedrock and stony subtypes) within the area, which will be used to assist with the development of management advice in relation to the areas and features designated for conservation. In addition, further evidence was acquired to define more accurately the transitional boundaries between coarse/mixed sediments in the northern and western areas of the cSAC, and to enable a better understanding of the distribution of sedimentary and reef habitats within the palaeovalley situated in the southeastern section of the survey area.

The survey was successful in acquiring multibeam, side-scan and ground-truthing data of the seabed. Although full data coverage of the whole cSAC was not possible in the time available, five areas were targeted for intensive survey, with 100% acoustic data coverage of these areas.

Given the predominantly hard nature of the seabed and the lack of differentiation in acoustic signatures between stony reef and coarse sediments, there was little potential to discriminate, and map different reef categories based on acoustic features. However, analysis of available data enabled the delineation of Annex I bedrock and boulder reef and confirmed that the concentration of bedrock reef is higher inside the cSAC boundary than outside.

The benthic community observed over the entire survey area was very diverse and variable in its distribution over a small spatial scale, with different variations of the whole assemblage arranged in an irregular mosaic across the entire area.

Although there are signs of human activity and physical disturbance still evident on the seabed, no evidence of sustained or permanent damage to the benthic assemblage was observed during this investigation.

Contents

1 Background and introduction

Wight-Barfleur Reef is an area of bedrock and stony reef located in the central English Channel, between St Catherine's Point on the Isle of Wight and Barfleur Point on the Cotentin Peninsula in northern France. The bedrock reef is characterised by a series of well-defined exposed bedrock ridges, up to 5m high, together with areas of flat, smooth mudstone and sandstone with overlying coarse sediment (gravels, cobbles and boulders), which in places forms stony reef. As such, the seabed conforms to the definition of Annex I Reefs within the EU Habitats Directive.

Approximately 21km south of the Isle of Wight, an area encompassing the extent of the reef has been proposed for designation as a candidate special area of conservation (cSAC; Figure 1), under the criteria for site selection outlined in Annex III of the Habitats Directive. A designated area remains a cSAC until it has been formally designated as a SAC by UK Government, following approval as a site of community importance (SCI) by the European Commission. The Wight-Barfleur Reef cSAC was submitted to the European Commission for consideration on 30 August 2012 and was still awaiting approval as a SCI at the time of report writing.

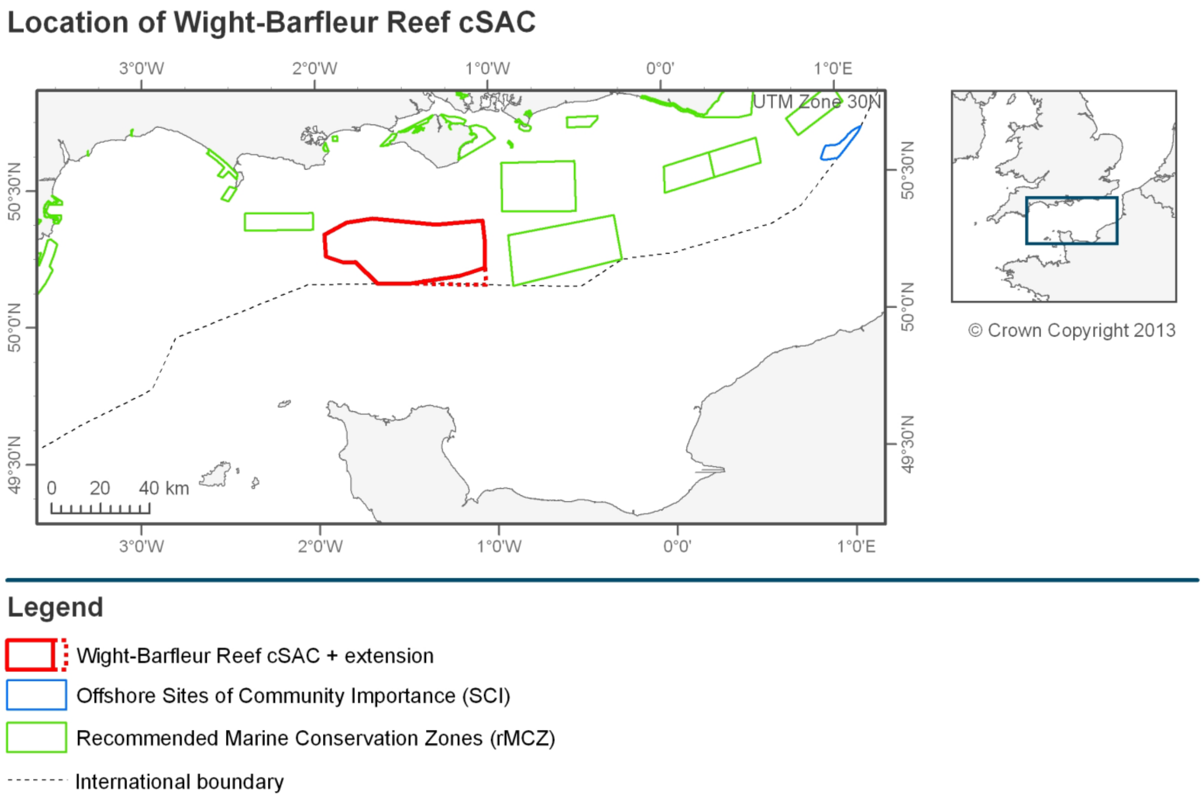

Figure 1. Location of the Wight-Barfleur Reef cSAC in relation to other Marine Protected Areas (MPAs).

The Wight-Barfleur Reef cSAC is approximately 65km long (east to west) and up to 26km wide (north to south). The depth within the cSAC ranges from 25m to 100m below Chart Datum (CD), with the deepest areas to the south, and within the palaeovalley, which runs along the southeastern edge of the cSAC.

A dedicated multidisciplinary survey of Wight-Barfleur Reef cSAC was conducted in March 2013 aboard the RV Cefas Endeavour. An area adjacent to the south-eastern boundary of the Wight-Barfleur Reef cSAC covering the seabed towards the international boundary (formerly the Wight-Barfleur Extension rMCZ) was also surveyed with the same vessel in February 2012. The purpose of both surveys was to acquire data to better delineate the extent of Annex I reef (both bedrock and stony subtypes) within the area, which could be used to assist with the development of management advice in relation to the areas and features designated for conservation. In addition, further evidence was acquired to define more accurately the transitional boundaries between coarse/mixed sediments in the northern and western areas of the cSAC, and to enable a better understanding of the distribution of sedimentary and reef habitats within the palaeovalley situated in the southeastern section of the survey area.

This report describes the findings from the analysis of data collected during the February 2012 (CEND0312) and March 2013 (CEND0313) surveys, combined where possible with relevant historical datasets.

2 Survey design and methods

2.1 Survey plan

A grid of ground-truthing stations spaced 5km apart was placed over the Wight-Barfleur Reef cSAC survey area and orientated in line with existing acoustic and ground-truthing data (Figure 2). At most stations on the grid, an underwater video tow was performed using a drop camera frame, and a 0.1m^2 mini-Hamon grab was deployed to collect benthic infauna and sediments (ground type permitting). Gridded stations from which historical benthic data already existed were excluded from further sampling. New multibeam acoustic data were collected during transits between sampling stations, as well as within each of five smaller survey boxes; these boxes were chosen to represent specific areas of interest within the Wight-Barfleur Reef cSAC. The rationale behind the placement of each intensely surveyed box is presented in Table 1. Data collected within boxes consisted of 100% coverage side-scan data and 50% multibeam (except for Box 1, which had 100% coverage of both data types). Additional ground-truthing stations were targeted based on the real-time analysis and field interpretation of newly acquired acoustic data. A large (0.25m^2) Hamon grab was used to acquire qualitative samples of cobble and of sponge specimens where appropriate.

Stations sampled, and opportunistic acoustic data acquired during the February 2012 survey covering the area to the southeast of the cSAC, do not correspond with the survey grid and are considered as additional ground-truthing stations.

Table 1. Rationale for the placement of each intensely surveyed box.

Box	Rationale
Box 1 Box 2 Box 3	These boxes represent transitions from a fished to non-fished area (based on non-UK demersal gear VMS data)
Box 4	Area of potential habitat complexity observed on the underlying Astrium DEM bathymetry – including some areas that were indicated from previous work as *potential* Annex I stony reef
Box 5	Area of the paleo-valley in the southern section of the site containing records of demersal fishing activity (based on non-UK demersal gear VMS data)

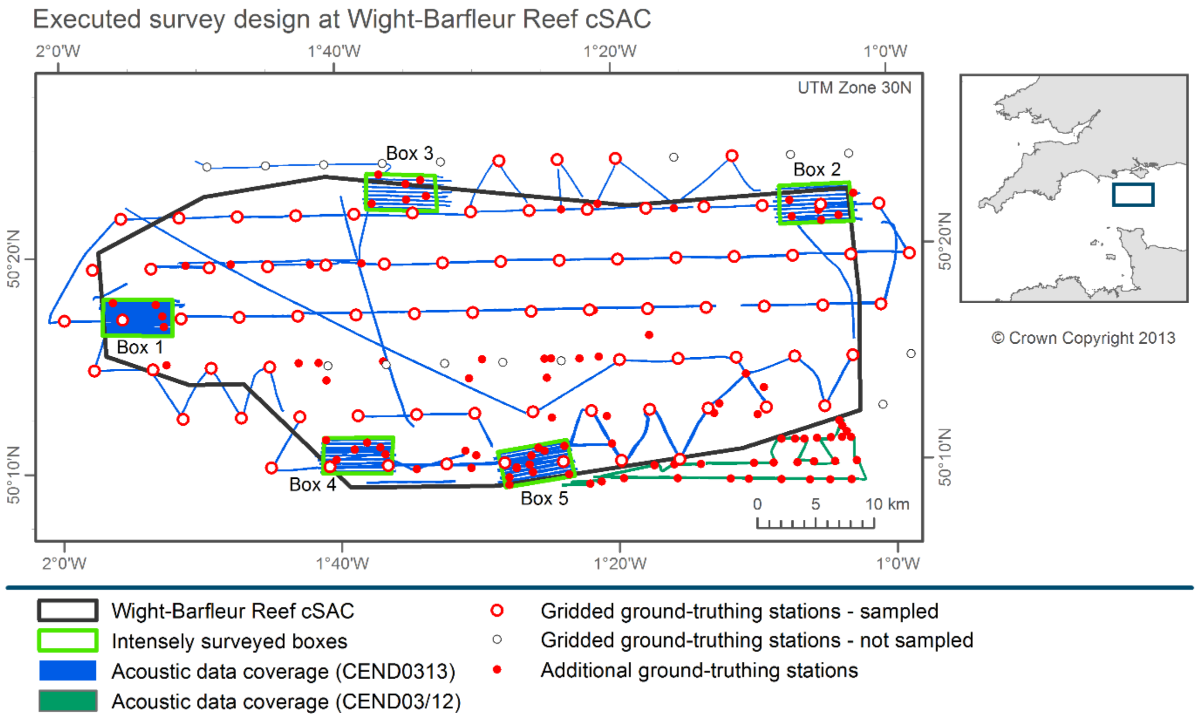

Figure 2. Acoustic and ground-truthing survey design executed at Wight-Barfleur Reef cSAC.

2.2 Acoustic and geophysical data acquisition

2.2.1 Side-scan sonar

An Edgetech FS-4200 dual frequency (300/600kHz) side-scan sonar was used in combination with the Edgetech Discovery software for data recording. Data were recorded in XTF format and post-processed using the Triton Imaging software suite (Isis and TritonMap). Layback was applied using High Precision Acoustic Positioning (HIPAP).

2.2.2 Multibeam echosounder

Data were collected using a Kongsberg EM2040 multibeam echosounder (MBES), Seapath 300 attitude sensor and CNAV 3050 high precision GPS. Bathymetry data were processed using CARIS HIPS and backscatter data were produced with the QPS FMGT software package. Variations of sound velocity with water depth were determined using a CTD (conductivity-temperature-depth) probe with a sound velocity profile (SVP) measurement taken at least once every 24h when collecting MBES data; acquired SVP data were applied during multibeam data acquisition.

2.3 Grab sample and seabed imagery acquisition

2.3.1 Sediment and biological samples

Sedimentary habitats were ground-truthed using a mini-Hamon grab on fine sedimentary substrates (sampling area: 0.1m^2), or a Hamon grab (sampling area: 0.25m^2) on coarser substrates. On recovery of the mini-Hamon grab, the sample was decanted into a container and a representative sub-sample of sediment (c. 0.5 litres) was removed for particle size analysis (PSA). The remaining sample was photographed, and the volume measured and recorded. The sample was washed with seawater over a 5mm mesh and a 1mm mesh sieve to separate the coarse material and fauna from the finer sediment. The retained material on both sieves was transferred into a pre-labelled sample container and fixed using a buffered 4% formaldehyde solution. Photographs were taken of the sediment fraction retained on both sieves (see Whomersley 2013). On recovery of the larger Hamon grab, any sponges present were removed from the cobbles and preserved in industrial methylated spirit (IMS). The remaining cobbles and attached fauna were preserved in buffered 4% formaldehyde solution.

2.3.2 Underwater video and photographic imaging techniques

Set-up and operation of the drop camera system followed the MESH 'Recommended Operating Guidelines (ROG) for underwater video and photographic imaging techniques'. The drop camera system comprised a video camera also capable of capturing still images. Illumination was provided by underwater lights and a flash unit. The camera was fitted with a four-spot laser-scaling device to provide a reference scale in the acquired image – red laser spots were 17cm apart in a square configuration in the centre of the field of view. The camera frame was controlled by a winch operator with sight of the video monitor. USBL positioning was used in addition to the starboard gantry offset to log the position of the drop camera during each deployment.

Video footage was recorded simultaneously to a Sony GV-HD700 DV tape recorder and a computer hard drive. A metadata overlay, including time and GPS position (of the vessel), was applied to the recorded video image. Camera deployments lasted a minimum of 10 minutes and were run at c. 0.5 knots (c. 0.25ms^{-1}) across a 200m 'bullring' centred on the sampling station or along a specific transect. Still photographic images were captured at one-minute intervals and opportunistically if specific features of interest were observed.

2.4 Sample processing and data analysis

2.4.1 Grab samples

Grab samples were processed for the extraction, identification and weighing of macrofauna by APEM Ltd following standard laboratory practices. Results were checked following the recommendations of the National Marine Biological Analytical Quality Control (NMBAQC) scheme (Worsfold *et al.* 2010).

For the present report, standard univariate and multivariate analyses have been performed on the taxon abundance-by-sample matrix generated by the grab sample processors. Prior to analyses, the data matrices were checked for inconsistencies and spurious entries (egg masses, fragments, *etc*.). Metrics calculated for each sample included total macrofaunal abundance (N), total wet weight biomass (B), total number of taxa (S) and Hill's (1973) taxon diversity index (N1). Multivariate analyses were performed using the PRIMER 6 software package (Clarke & Gorley 2006). These analyses included calculations of faunal similarity using the Bray-Curtis similarity coefficient applied to square-root transformed abundance data. Sample clustering techniques (SIMPROF) were also employed to identify statistically significant groups of samples and the SIMPER routine was performed to identify which taxa contributed to the similarity between statistically defined groups.

2.4.2 Video and stills analysis

Acquired video and photographic stills from within the Wight-Barfleur cSAC were processed by Thompson Unicomarine Ltd, whereas those acquired in 2012 from the Wight-Barfleur cSAC extension in the southeastern corner were processed at Cefas. Data from the original analysis of video and stills from the 2006 survey were also used. All datasets were processed in accordance with the guidance documents developed by Cefas and JNCC for the acquisition and processing of video and stills data (Coggan & Howell 2005; JNCC, in prep.). The report created by Thompson Unicomarine (Owen *et al*. 2013) is available on request. No dedicated report was created internally by Cefas' processors.

2.4.3 Cobble epifaunal analysis

Fauna attached to cobbles retained from sampling the seabed with the large Hamon grab have been identified by APEM Ltd. These data, from seven stations, have been used to assist in the verification of the identity of taxa observed on the video footage and still images. They remain, however, qualitative examples, and as such, no formal community analysis has been performed on them.

2.4.4 Particle size analysis

Particle size analysis (PSA) was carried out by Cefas following standard laboratory practice and the results were checked by specialist Cefas staff following the recommendations of the National Marine Biological Analytical Quality Control (NMBAQC) scheme (Mason 2011). PSA data have been analysed in conjunction with benthic faunal datasets where appropriate to elucidate any possible correlations between the two datasets. Detailed descriptions of specific analyses are presented in context, below.

2.4.5 Acoustic data preparation

MBES data layers (bathymetry and backscatter) were merged with data outputs from project ME1102 "Mapping Annex I Reefs in the central English Channel: evidence to support the selection of candidate SACs" (Coggan *et al*. 2009, data collected in 2006). Since bathymetry data from the 2012 and 2013 surveys related to Chart Datum (CD), and those of the 2006 survey related to mean sea level, it was necessary to transform the 2006 dataset. Areas of overlap between bathymetry data from the discrete surveys were identified and 1000 random sample points selected within these areas. Bathymetry values from both raster surfaces were extracted at these sample points and values plotted against each other. A strong and statistically significant correlation was found and used for transformation of the 2006 dataset from mean sea level to CD. The same procedure was applied to the discrepant backscatter datasets, which showed differences as a result of the multibeam system upgrade onboard RV *Cefas Endeavour* (from Kongsberg EM3002D in 2006 to Kongsberg EM2040 in 2013). This yielded a much weaker, though still statistically significant, relationship that was used for transformation. Both data layers were projected to UTM 30N at a resolution of 5m.

Several derivatives were calculated from the bathymetry raster, including slope, two roughness layers with kernel sizes of 3x3 and 9x9, eastness, northness, profile curvature, planar curvature, combined curvature and the bathymetric position index (BPI) with radii of 3, 5, 10 and 15 cells.

As the MBES data did not give full coverage of the seabed, the Defra 1 arcsec digital elevation model (DEM) was also used where necessary. The original dataset was clipped to the study site and projected to UTM 30N at a resolution of 25m, which equates to 1 arcsec at the latitude of the study site.

2.4.6 Acoustic data interpretation

Initially it was envisaged that a sample-based analysis in an object-based image analysis (OBIA; Blaschke 2010) framework would be conducted with conditional inference trees (Hothorn *et al*. 2004) employed as a classifier. Therefore, all available video and grab sample data from all surveys (2006, 2012 and 2013) were combined and classified into relevant Annex I categories (bedrock reef, biogenic reef, stony reef and not reef). The assignments were used to inform the semi-automated process of map production using OBIA implemented in the software package eCognition v8.9.

OBIA is a two-step approach consisting of image segmentation and classification. The segmentation divides the image into meaningful objects based on their spectral and spatial characteristics. The resulting objects can be characterised by their various features, such as layer values (mean, standard deviation, skewness, *etc*.), geometry (extent, shape, *etc*.), texture and many others. The subsequent classification of the objects is based on combinations of these features.

Segmentation was carried out employing the ‘multiresolution segmentation’ algorithm in eCognition. This is an optimisation procedure that starts with an individual pixel and consecutively merges it with neighbouring pixels to form an object. The process continues until a threshold value for a scale parameter is reached, the threshold being determined by the operator.

The multi-resolution segmentation was carried out at pixel level on backscatter strength and BPI15. In a subsequent step, small objects (less than four pixels) were merged with neighbouring objects with similar spectral characteristics. Finally, neighbouring objects were merged as long as their difference in backscatter strength and BPI15 remained below a predefined threshold using the ‘spectral difference segmentation’ algorithm. In this way, the number of objects was reduced.

For every image object that coincided with a ground-truthing sample, object mean values of acoustic data layers were exported as a .txt file. Box-plots of object mean values of primary (bathymetry and backscatter) and secondary (derivatives as mentioned above) raster layers by Annex I sub-type were plotted based on these extracted values. A conditional inference tree was grown to find significant thresholds in the data.

This approach did not yield meaningful results. The two most likely reasons for this are (i) the small-scale habitat heterogeneity at a spatial scale equal to or smaller than the positioning accuracy of the ground-truthing equipment or (ii) the limitations of the acoustic systems to differentiate between the closely related seabed types. Consequently, it was decided to employ an alternative approach that would be less reliant on sampling data and would take into account pre-existing local knowledge of the area and general principles relating to geomorphology, geology and habitats.

Collier *et al*. (2006) found that seabed morphology and bathymetric texture were directly related to bedrock geology in the central English Channel south of the Isle of Wight. Diesing *et al*. (2009) made use of these relationships to map the rocky reef in the same area. The same authors mapped areas of seabed where bedrock ridges occurred as bedrock reef; however, they made no attempt to further differentiate bedrock ridges from flat rocky seabed and depressions in the bedrock which are likely to be covered by a thin veneer of sediment.

Protuberances from the seabed, which are most likely bedrock ridges within the study site, can be mapped with a BPI of suitable scale factor, which should be of a similar size as the features to be mapped. A neighbourhood size of 125m was found to give the best results. This translates into a scale factor of 25 (25 (scale factor) x 5m (resolution) = 125m) for the MBES dataset and 5 for the Defra DEM. The respective BPIs were calculated from the two bathymetric datasets and subsequently merged. The combined data layer was classified into three classes using Jenks natural breaks: Negative BPI values <-0.54 indicate depressions, BPI values in the range from -0.54 to 0.37 highlight flat or gently sloping seabed and positive BPI values >0.37 identify positive seabed expressions such as ridges and crests. The latter class was assumed to be a satisfactory representation of bedrock ridges within the study site.

Side-scan sonar data collected at the five intensely surveyed boxes were used in conjunction with the multibeam bathymetry and backscatter data to enable the expert manual interpretation of the Annex I stony reef contained within. The ESRI ArcGIS v9.3.1 software package was used as a tool for delineating distinct sediment changes within the boxes.

Initially, only Annex I features, comprising rocky and stony reef, were to be identified and mapped from the side-scan record. However, as stony reef was not found to have a unique signature on the side-scan record, delineating stony reef (comprising of stable cobbles and boulders) was not always possible. Due to the larger size of the particles involved, boulder reefs could be identified easily from the side-scan sonar record. Where ground-truthing data showed both stony reef and no reef to be present, but no distinction was possible from the acoustic record, areas of the seabed were classed as mosaic substrates. In these areas, a mixture of stony reef and coarse or mixed sediment types are believed to be present, in unknown proportions. Areas where bedrock was exposed at the seabed surface could be identified and delineated from the multibeam and side-scan records, as well as areas with sedimentary bedforms. In some areas the acoustic record revealed complex detail of the features present. Where features were less than $600m^2$, they were not delineated individually but considered as part of the wider feature observed. Ground-truthing data were used to aid the interpretation of acoustic data.

2.5 QA/QC

All ground-truthing activities in the field were performed according to the recommendations in the following documents:

- Biological Monitoring: General Guidelines for Quality Assurance document
- Quality Assurance in Marine Biological Monitoring[1]
- Recommended operating guidelines for underwater video and photographic imaging techniques[2]

Reports generated from the QA of the biological data generated for this study are listed in Appendix 3.

3 Results and Discussion

3.1 Multibeam bathymetric and backscatter maps

Figure 3 shows the bathymetry within the study site based on the 1 arcsec Defra DEM. Water depths range from 32m to 101m below CD. Visible are the different bathymetric textures with areas of smooth seabed predominantly north and west of the Wight-Barfleur Reef cSAC boundary and rougher seabed, displaying a series of closely spaced ridges up to 5m high and several kilometres long within the cSAC boundary. Also visible is the Northern Palaeovalley, approximately 100km long, running from northeast to southwest.

Figure 4 and Figure 5 show the merged MBES bathymetry and backscatter datasets from the 2006, 2012 and 2013 surveys.

[1] Reference URL: http://www.nmbaqcs.org/qa-standards/qa-in-marine-biological-monitoring.aspx
[2] Reference URL: http://www.searchmesh.net/PDF/GMHM3_Video_ROG.pdf

Analysis of the extracted object mean values of bathymetry, backscatter and derivatives for the four categories of Annex I reef (bedrock reef, biogenic reef, stony reef, not reef) revealed that there was little potential to discriminate and map different reef categories based on acoustic features (Figure 6). In most cases there was significant overlap of value ranges for the different reef categories. This is confirmed by the conditional inference tree that was grown based on the same data sets (Figure 7). The terminal nodes (at the bottom of Figure 7) show a high degree of impurity, which means that a reliable distinction between the different reef categories is not possible. This is particularly true for the stony reef category, and confirms the observations made from the side-scan sonar records. Potential reasons why it was difficult to discriminate the different categories of Annex I reef are explored under Section 3.9.

Results of the terrain analysis employing a BPI with a neighbourhood size of 125m are shown in Figure 8. The terrain class 'ridges' was assumed to represent Annex I bedrock reef within the study site, and the spatial distribution of bedrock reef thus defined is shown in Figure 9. It is apparent that the concentration of potential bedrock reef is considerably higher inside the cSAC boundary than outside; the contrast being especially noticeable on either side of the northern boundary. Within the cSAC boundary, outcrops of potential bedrock reef are spread throughout the entire area.

Generally, the pattern of bedrock reef distribution is determined by bedrock geology (Figure 9). Jurassic and Lower Cretaceous bedrock comprise a varied and partly cyclic lithology, displaying a differential resistance to erosion. As the strata were subsequently folded and tilted, they developed into a series of ridges and intervening troughs through differential erosion. Conversely, where soft and uniform Upper Cretaceous chalk is present at the seafloor, the seabed is flat and smooth, and bedrock reef is largely absent. Where the Northern Palaeovalley has cut through the different strata, bedrock reef is found at the steep slopes of the valley, with the most prominent structures present in bedrock of Palaeogene age.

3.2 Side-scan sonar maps

Distinctive acoustic signatures present on the side-scan mosaics include complex patches of high and low intensity returns. Areas of higher side-scan backscatter (darker tones) and lower backscatter (light tones) are interspersed with areas with a mixture of the two, making up the main sediment constitute classed as mosaic (incl. stony substrates).

Figure 10 presents an overview of the side-scan sonar data collected during the 2013 survey. Side-scan sonar returns are not uniform throughout the Wight-Barfleur Reef cSAC, indicating a heterogeneous seabed dominated by rocky and stony reef. The data acquired from each intensely surveyed box is considered in detail, in turn, below.

Box 1

Side-scan data from Box 1 revealed a seabed featuring parallel longitudinal furrows (Figure 11). Seabed furrows have been recorded around the British Isles on gravel, sand and mud substrates (Stride *et al.* 1982). Such features in the western English Channel have been defined as longitudinal furrows in loose gravel and pebbles (Holme & Wilson 1985). These furrows form in parallel lines aligned with the strong tidal stream (>150cm s^{-1}) and are oriented northeast to southwest on a gravel substrate (Reading 1996).

Video footage acquired during the 2013 survey indicated that the observed features corresponded to strips of sand or gravel to one side of a rock furrow and mixed pebbles/ cobbles to the other. The furrows varied in dimension but were typically between 50-100m apart and were associated with exposed bedrock reef. It is thought that bottom currents are likely to have removed sand from the furrow area resulting in a residue of heavier gravel being left behind.

Figure 12 identifies three distinct side-scan sonar backscatter signatures observed within Box 1, including furrows, coarse sediment and bedrock. Due to the difficulty in mapping furrows individually, it was deemed appropriate to class the entirety of Box 1 as a mosaic, which includes bedrock and stony reef. Figure 13 presents the interpreted mosaic layer.

Box 2

According to the side-scan data, Box 2 comprised a complex mixture of sand, bedrock and a mosaic of stony reef, bedrock and coarse sediment, as illustrated in Figure 14. The seabed was characterised by bedrock outcrops with areas of sand mega-ripples situated to the east and west. The remaining seabed was predominantly a mosaic substrate, including stony reef and coarse sediment, with a boulder field observed in the southern half of the box. Examples of the observed ground types are provided in Figure 15 and their distribution is presented in Figure 16.

Box 3

Data from Box 3 indicate that the seabed comprised a mosaic of stony reef, bedrock and coarse sediment (Figure 17). The side-scan sonar signature indicated a mosaic that included stony substrate (Figure 18). The southwestern area of the box had a mixture of stony reef with swathes of sand mega-ripples and boulder fields. To the east, an area of bedrock outcrop was observed, interspersed with sand waves. Example signature types can be seen in Figure 18, including sand waves and ripples, bedrock and boulder fields. The boulders, in particular, have a clear and distinct return on the seabed imagery within Box 3.

Box 4

Side-scan data from Box 4 displayed a relatively homogenous seabed signature, indicating a mosaic of substrates including stony reef and coarse sediment (Figure 20). Figure 21 depicts three side-scan sonar signatures within Box 4, namely sand, stony reef and coarse sediment. Areas of mixed intensity return have been classed as mosaic (incl. stony substrates) in the interpretation (Figure 21). There were also small patches to the northern section of the site where sand waves occurred (Figure 22).

Box 5

Box 5 was comprised of mosaic substrate interspersed with sand waves, bedrock and a large area to the west containing boulder fields. The intensity of the side-scan sonar data was slightly higher towards the west (Figure 23), indicative of a harder substrate, such as pebbles, cobbles and boulders. There were bedrock outcrops in the eastern part of the box (Figure 24) and an acoustic signature characteristic of that created by reef building organisms. However, although the side-scan signature indicated such a feature, the still images from this area did not confirm the presence of taxa known to create biogenic reef, such as *Sabellaria spinulosa* or mussels (Figure 25).

3.3 Surficial sediments

Since much of the seabed in the area of interest was unsuitable for sampling using a grab, only limited quantitative data exist on the surficial sediments of the Wight-Barfleur Reef cSAC. Fourteen grab samples were available for the extraction and quantitative analysis of particle size distribution data. From the data generated, samples have been classified according to both the modified Folk and the EUNIS sediment classification systems (Long 2006). All sediment samples collected contained at least a fraction of gravel-sized sediments (Figure 26), resulting in a classification of 'coarse sediment' under the EUNIS classification system across stations. The proportion of this gravel fraction relative to other sediment particles determined the precise description allocated under the modified Folk classification system; samples ranged from the predominantly fine 'gravelly sand' to the uniformly coarse 'gravel'. Most samples were classified as 'sandy gravel' (Figure 26).

Table 2. Summary of sediment descriptions from stations successfully sampled for PSA. Substrate descriptions from video footage of the same stations provided for comparison.

	Grab sample PSA result		Video sample substrate description
Station	Folk classification	EUNIS classification	EUNIS code & MNCR Descriptor
HP_07	Gravelly sand	Coarse sediment	No sample
HP_09	Sandy gravel	Coarse sediment	A4.1/2 – High/moderate energy circalittoral rock
HP_22	Gravel	Coarse sediment	A5.13 – Infralittoral coarse sediment
HP_30	Sandy gravel	Coarse sediment	A5.14 – Circalittoral Coarse Sediment
HP_31	Gravel	Coarse sediment	A5.14 – Circalittoral Coarse Sediment
HP_37	Gravel	Coarse sediment	A5.14 – Circalittoral Coarse Sediment
HP_39	Sandy gravel	Coarse sediment	A5.14 – Circalittoral Coarse Sediment
HP_42	Sandy gravel	Coarse sediment	A5.14 – Circalittoral Coarse Sediment
HP_43	Sandy gravel	Coarse sediment	A5.14 – Circalittoral Coarse Sediment
HP_45	Sandy gravel	Coarse sediment	A5.14 – Circalittoral Coarse Sediment
HP_48	Sandy gravel	Coarse sediment	A5.14 – Circalittoral Coarse Sediment
MP_03	Sandy gravel	Coarse sediment	A5.2 – Sublittoral sands and muddy sands
MP_17	Sandy gravel	Coarse sediment	A4.1 – High energy circalittoral rock
MP_19	Sandy gravel	Coarse sediment	A5.14 – Circalittoral Coarse Sediment

Substrate descriptors from the video footage at each of the grabbed stations broadly coincided with the 'coarse sediment' result from PSA. Only two of the descriptors from the video footage – describing rock – contradicted the result from PSA. The discrepancy is likely to be a result of differences in scale; the broad-scale substrate observed on the video conforming to a predominantly rocky habitat, with localised areas of sediment which were successfully sampled with a grab.

3.4 Infauna

Fourteen grab samples were available for extraction and quantitative analysis of infauna. The relatively low number of grab samples obtained relative to the total number of sampling stations is a reflection of the hard substrate characterising the survey area, which is unsuitable for grabbing. Results from analyses performed on this reduced infaunal dataset are informative but of limited value when trying to identify area-wide patterns in benthic community structure.

Table 3 summarises the assemblage metrics derived from each grab sample.

Table 3. Assemblage metrics derived from each grab sample obtained from the Wight-Barfleur Reef cSAC.

Sample	No of taxa	Biomass (ww g)	Abundance	Diversity (N1)	Evenness (N21')
MP_03	4	0.0293	3	3.00	1.00
HP_07	9	0.0060	9	6.24	0.84
HP_39	12	0.9539	14	8.74	0.84
HP_43	14	0.0595	18	11.90	0.90
HP_37	18	0.7774	22	12.48	0.79
HP_09	27	0.5632	28	20.04	0.88
HP_45	34	2.4550	50	16.73	0.48
MP_17	41	1.8294	104	11.50	0.32
MP_19	41	38.8431	126	8.75	0.42
HP_31	44	1.0126	67	26.09	0.72
HP_42	55	4.1788	252	13.86	0.31
HP_48	60	18.6388	149	20.78	0.45
HP_22	72	6.7788	282	18.44	0.33
HP_30	100	4.8418	551	37.49	0.53

The spatial distribution of the total number of taxa recorded in each sample is illustrated in Figure 27. The variability in – and distribution of – most other metrics closely matches that observed for the total number of taxa.

The variability in proportion of the silt/mud fraction within sampled sediments showed the highest correlation with the variation in the number of infaunal taxa, their abundance and their biomass (data not shown); samples with a higher proportion of silt/mud also harboured a greater biomass, abundance and number of taxa. Other sediment fractions showed no correlation with the variability in the assemblage metrics recorded.

Multivariate analysis of square root transformed infaunal abundance data revealed five statistically distinct assemblages, three of which represented by a single sample (see insert at bottom of Figure 27). Three of the five distinct assemblages were represented by a single station (assemblages a, b and c). The remaining two assemblages (d and e) were represented at several sampling stations each (Figure 27). Taxa characterising each assemblage represented by more than one sample are listed in Appendix 1.

3.5 Epibenthos

Epibenthic data have been obtained from the processing of video footage (172 samples from the same number of stations), still photographs and cobble samples. Organisms have been identified to the lowest possible level given the quality of the visual evidence available. Often, organisms could only be identified to the level of phylum (e.g., Porifera) but classified further using a descriptor of life form (e.g., columnar, encrusting). The newly acquired dataset was combined with that created from the analysis of relevant historical datasets, and after rationalisation (i.e., identification and truncation of duplicate and spurious entries), a single dataset containing 213 taxa was obtained.

Traditional quantitative statistical analysis of these data is not advisable given the uncertainty in the precise identity of the organisms recorded. Any potential patterns in community composition derived from such analyses would be reliant upon assumptions on the uniqueness and independence of taxa from one another. Such assumptions cannot be guaranteed when using the available data. For example, a single species of sponge may display a different form depending on where it lives, yet each life form recorded for that species would be considered a separate species, thus distorting the perceived community composition and diversity of an area. Equally, the same life form recorded from different samples (e.g., solitary Ascidiacea) may be representative of several different species within that taxon. Instances like these are present in all benthic datasets, but when the majority of data records within a dataset comprise such entries, the uncertainty surrounding the validity of any pattern observed following their analysis is too high to be reliable. Because of this, analyses of epibenthic assemblage composition have been performed on a presence/ absence list of recognised taxa recorded from both still images and video footage. Such data may be used to attain an idea of variability in assemblage across the survey site but must not be relied upon to attain a definitive or quantitative benthic characterisation of the area. Multivariate analyses revealed 30 statistically distinct groups of sampling stations (i.e., assemblages labelled a to z and aa to ad thereafter; Figure 28). The largest difference in similarity between distinct assemblages was underpinned by the three different datasets that contributed to the whole dataset analysed (i.e., datasets from the 2006, 2012 and 2013 surveys were separated statistically, highlighting the overriding influence of unavoidable differences in video and still sample processing between the analysts of each dataset). Therefore, the exact distribution of each distinct assemblage must not be afforded undue importance or ecological legitimacy.

Within the apparently random distribution of identified distinct assemblages, one pattern that can be discerned is a vague transition in overall assemblage composition from west to east (Figure 28). Towards the west, stations belong predominantly to distinct assemblage e (coloured orange), whereas towards the east, stations belong predominantly to the distinct assemblages r and s (coloured red). There is no spatial overlap between these assemblage pairs. There is also a trend in increasing taxon richness from west to east, as evidenced by the greater occurrence of larger circles (denoting the number of taxa recorded at each station) towards the east of the survey area than towards the west (Figure 28). Broad-scale longitudinal changes in benthic assemblage composition have been observed before in the central and eastern English Channel, albeit for fauna collected using a grab (Coggan *et al*. 2012).

The apparent clustering of assemblages u, x, y and z in the south-eastern corner of the survey area is an artefact of sample processing; these stations were all sampled in 2012 and the video samples processed by the same analyst. Equally, assemblages aa, ab, ac and ad, which cluster around the centre of the cSAC and consistently show a relatively lower taxon richness than the surrounding stations, were sampled and processed in 2006.

Intensely surveyed boxes 1, 2 and 3, towards the north of the survey area all contained samples representing assemblage q, the second most taxon rich assemblage (after assemblage s). Boxes 4 and 5 on the southern edge of the cSAC boundary were characterised predominantly by assemblages t and n respectively. Taxa contributing the most to the similarity within distinct assemblages represented by more than a single station are listed in Appendix 2.

During the analysis of the acquired video footage, whole video transects may be divided into segments should a distinct change in substrate or assemblage be observed along a transect. Multivariate analyses conducted on taxon presence data by video segment were conducted, resulting in the designation of 52 statistically distinct groups of segments. No discernible pattern in the distribution of these distinct groups was observed across the survey area. Correlation tests between physical and biological datasets corresponding to each video segment (i.e. RELATE and BIOENV routines in Primer) were also inconclusive, revealing no significant correlation between the two datasets. These results reinforce the notion of small-scale heterogeneity in assemblage composition across the mosaic of substrate types in the survey area, as well as the inability to predict epibenthic assemblage composition on seemingly different substrate types. Results of these analyses are not presented further.

3.6 Annex I habitats

Results have been combined from terrain analysis, manual interpretation of side-scan sonar data and information on stony reef gathered during previous work (Figure 34 in Coggan *et al.* 2009). The distribution of Annex I bedrock and stony reef at Wight-Barfleur Reef cSAC is shown in Figure 29. It is apparent that Annex I reef habitat is present throughout most of the designated area, interspersed with pockets of sediment veneer and exposed flat bedrock. Results from the analysis of epifauna would suggest that the benthic community of the whole area investigated is arranged as a mosaic of distinct assemblages, sharing many of their constituent taxa in varying ratios depending on the nature of the substrate and localised variations in exposure to prevailing currents. It would seem prudent to consider these statistically distinct assemblages as one coherent and interdependent benthic ecosystem, given the apparent lack of discernible boundaries between distinct assemblages.

3.7 EUNIS habitats

The new evidence on the distribution of habitats derived from terrain analysis and interpretation of side-scan sonar data was used to update the existing EUNIS habitat map of the Wight-Barfleur Reef cSAC and surroundings (Diesing *et al.* 2009). Previously, the study area was depicted as an extensive area of high-energy circalittoral rock surrounded by circalittoral and deep circalittoral coarse sediment. This interpretation relied heavily on Seazone Digital Survey Bathymetry data (a product similar to the Defra DEM). The authors noted that thin sediment veneers over flat bedrock occurred in places but were only distinguishable from high-resolution MBES data. They also noted that there was evidence from video footage that the steep walls of the palaeovalley exhibited rock; the areas were however too small to be mapped at the chosen map scale.

The interpretation of acoustic and video data presented here points to a highly complex seabed habitat, made up of a mosaic of bedrock reef, stony reef, coarse sediment and, in places, sand. To reflect the character of the seabed habitats better at the presented scale, the area previously mapped as high-energy circalittoral rock has been reclassified to X33 – Mosaics of mobile and non-mobile substrata in the circalittoral zone. However, information on the distribution of rock gained by terrain analysis was retained and is displayed as A4 – Circalittoral rock and other hard substrata. Video interpretation indicates that both high-energy and moderate-energy circalittoral rock occur. The spatial distribution does, however, show no relation to broad-scale patterns of modelled seabed energy (EUSeaMap; Cameron & Askew 2011). It is likely that small-scale variations in hydrodynamic energy, linked to topography causing local shading effects and acceleration of currents, are responsible for the observed pattern. Information from side-scan sonar was also included; bedrock and boulder fields were classified as circalittoral rock; sand was translated to A5.2 Subtidal sand. A more detailed assessment at EUNIS level 4 was not possible, as no information on sediment composition was available; however, it is unlikely that muddy sand is present in the study area due to the high-energy regime. The sandy habitats observed could be most likely classed as A5.25 Circalittoral fine sand and A5.27 Deep circalittoral sand (in the palaeo-valley). The resulting map is shown in Figure 30.

3.8 Anthropogenic impacts

Evidence of anthropogenic activity and disturbance to the seabed within the Wight-Barfleur Reef cSAC was observed in the form of marine litter and as trawl tracks. The most prominent example of marine litter observed was an upright shipwreck approximately 120m long captured on side-scan within the intensely surveyed Box 2 (Figure 31). Public records indicate this is possibly the wreck of the Meandros, which sank in 1934. Many other wrecks are known to occur within the Wight-Barfleur Reef cSAC boundary (Figure 32), although none of these was observed directly during the 2013 survey.

Other examples of marine litter were anecdotal observations of man-made materials from the acquired video and stills records (e.g., Figure 33).

Trawl marks left by fishing activities were observed in three of the five intensively surveyed boxes, namely Box 1, 3 and 5. Figure 34, Figure 35 and Figure 36 present the side-scan sonar imagery showing detailed trawl scar signatures. There is no way of knowing the age of such markings. In Box 1 the seabed to the northeast becomes sandier, which could be a reason why this area can be targeted for trawling. In Box 3, the orientation of trawl marks appears to be related to the predominant direction of the tidal stream, as the orientation of bed form scour and sand waves indicate a similar direction to the trawl scars. All scaring occurs within the stony reef mosaic layer. In Box 5 the direction of most trawl scars is mainly down to the predominant current direction in the area. The heavily fished patch to the south appears to be less stony and consist of coarse gravel with sand patches.

3.9 Data limitations

Initially, it was envisaged to base the mapping of Annex I reef habitats on a statistically robust analysis, linking categorical ground-truth sample information with acoustic features; however, this approach was unsuccessful. Several reasons might account for this.

Firstly, it appears that a significant amount of seabed is characterised by an intricate, small-scale mosaic of different habitats, including bedrock reef, biogenic reef, stony reef, coarse sediment and sand as evidenced by the analysis of side-scan sonar data from the survey boxes. Video footage of the seabed confirms such observations. Such a high spatial variability of habitat types requires an extremely high standard of positioning accuracy in order to yield meaningful results. Even small errors in geo-location might lead to incorrect associations between habitat category and acoustic features.

Secondly, although it would appear relatively straightforward to distinguish between bedrock and sediment, the matter is more complicated where a thin veneer of sediment occurs on top of bedrock. Likewise, cobbles could be interpreted as ‘reef’ where they provide a stable substrate or coarse sediment where they are mobile. This indicates that classification boundaries between reef and non-reef are fuzzy rather than crisp. As a consequence, classifications will vary to some degree depending on the individual who is carrying out the analysis, as classification of seabed imagery is not an objective approach.

Thirdly, not every distinction that can be made based on visual (video or stills) data has a representation in the relevant acoustic datasets. For example, cobbles will have near-identical acoustic signatures (MBES and side-scan) regardless of whether they are stable (reef) or mobile (coarse sediment), and equally the acoustic signature will be similar to that of pebble and coarse gravel substrates. Likewise, a thin veneer of sediment on top of rock might be penetrated by the acoustic pulse sent out by the sonar, giving the impression of a rocky substrate. All these factors might have contributed to the inability to discriminate the different reef types based on acoustic data in a statistically robust way, and similarly, they presented difficulties when undertaking expert interpretation, requiring areas to be described as mosaic habitats.

From a biological perspective, the scarcity of strictly quantitative benthic abundance data makes robust characterisation of benthic assemblages and communities more of a challenge. Reliance on photographic and video evidence can introduce discrepancies in the identification of certain taxa, and such discrepancies, if not recognised, may result in an inflated perception of assemblage diversity. It also means that a repeat survey of the same area, or even a repeat interpretation of the same data by a different analyst, may yield slightly different results. Therefore, any pattern described in the present investigation must not be relied upon too heavily for detailed, small-scale spatial management.

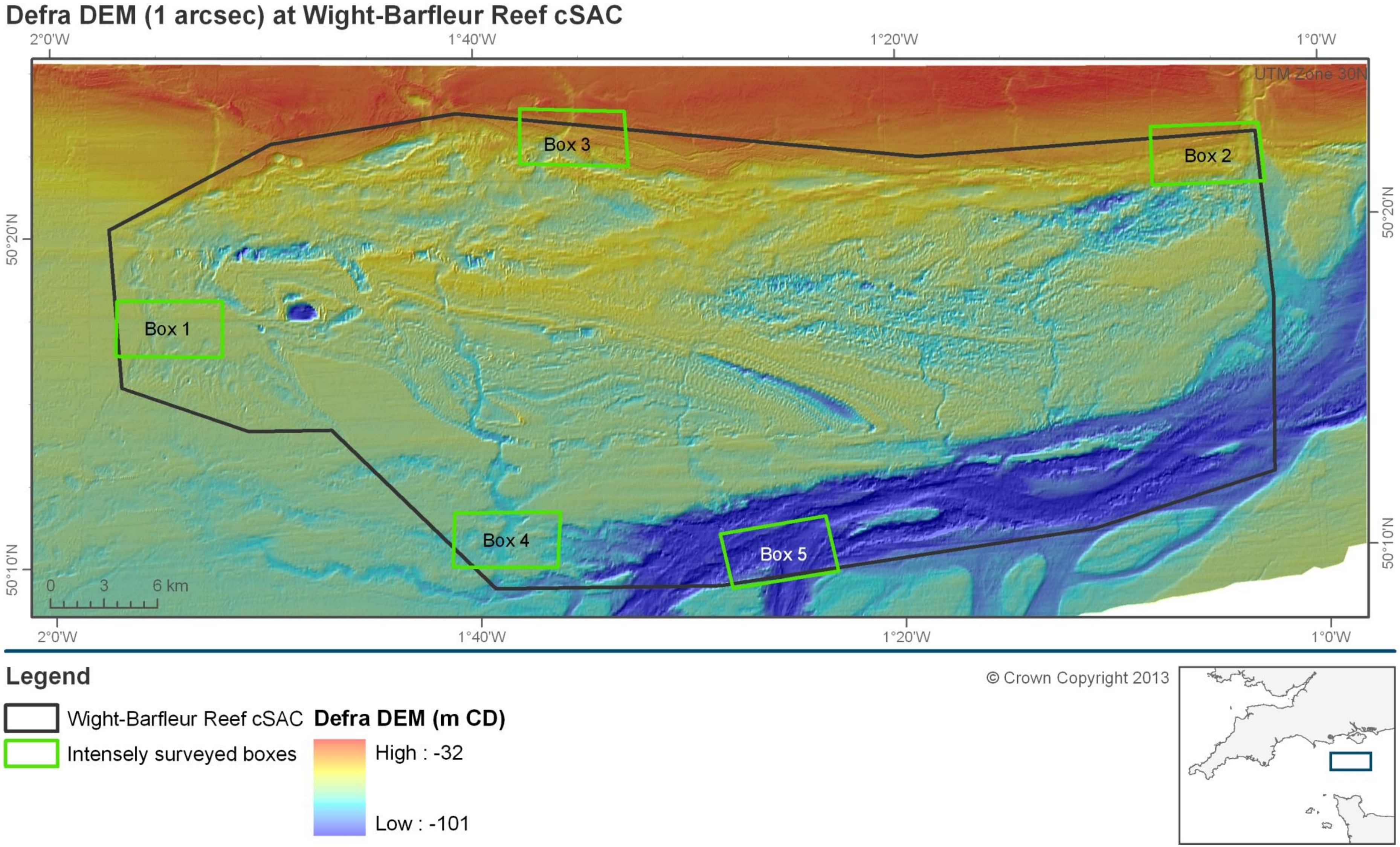

Figure 3. Bathymetry relative to CD within the study site based on the 1 arcsec Defra DEM.

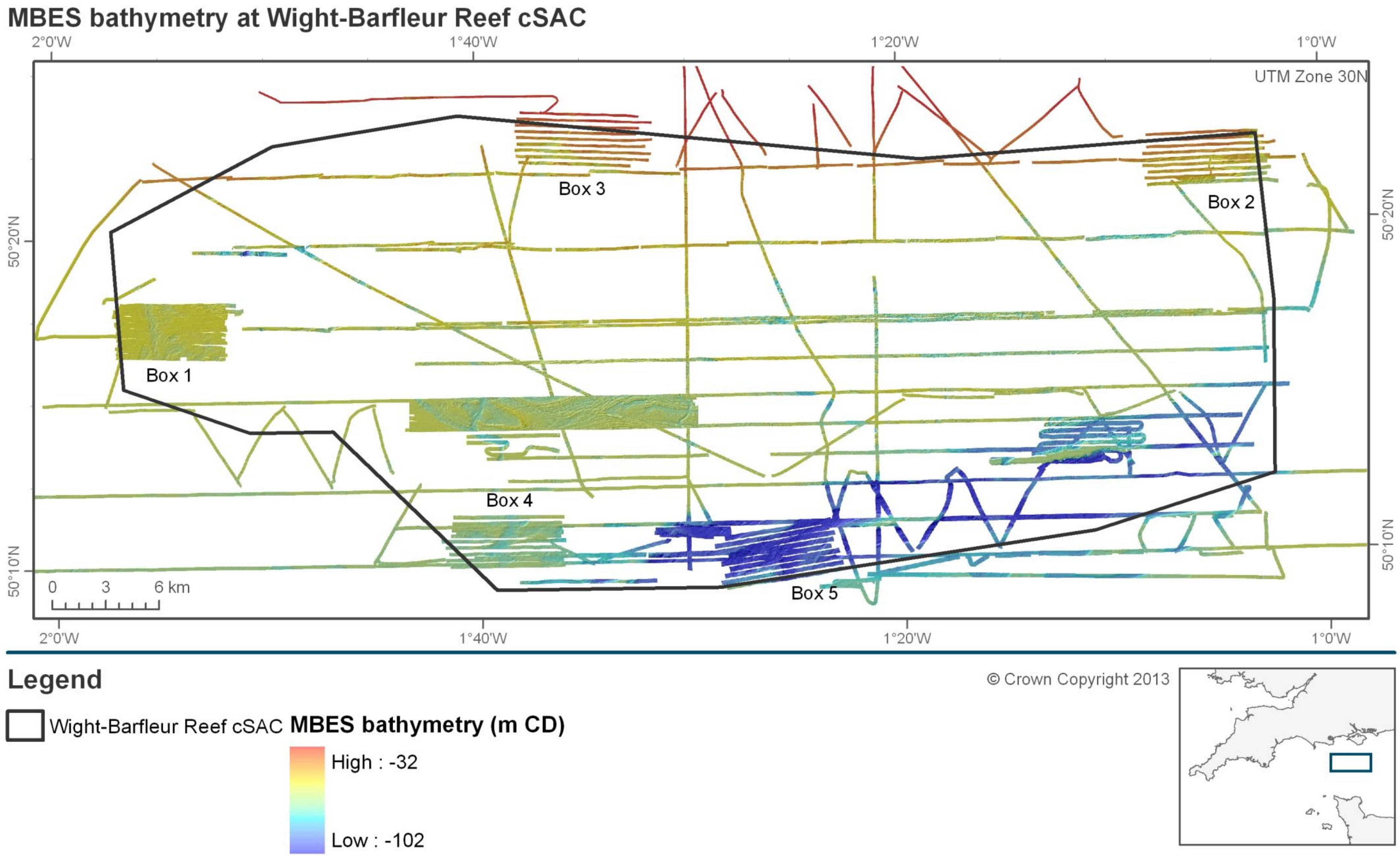

Figure 4. MBES bathymetry relative to CD within the study site based on the current surveys (2012 & 2013) and results published in Coggan *et al*. (2009).

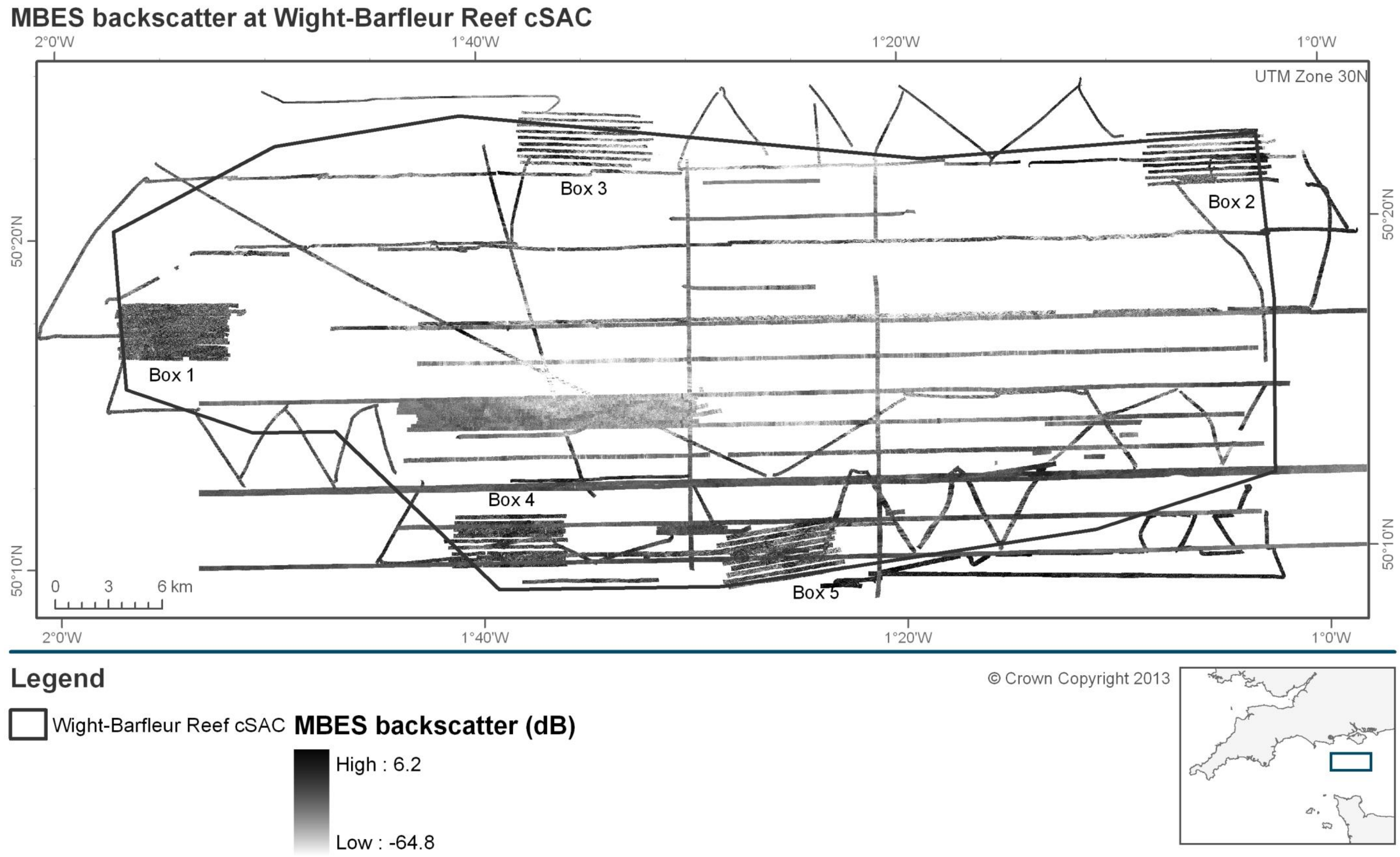

Figure 5. MBES backscatter data within the study site acquired on the dedicated surveys of 2012 and 2013, combined with data presented in Coggan *et al*. (2009).

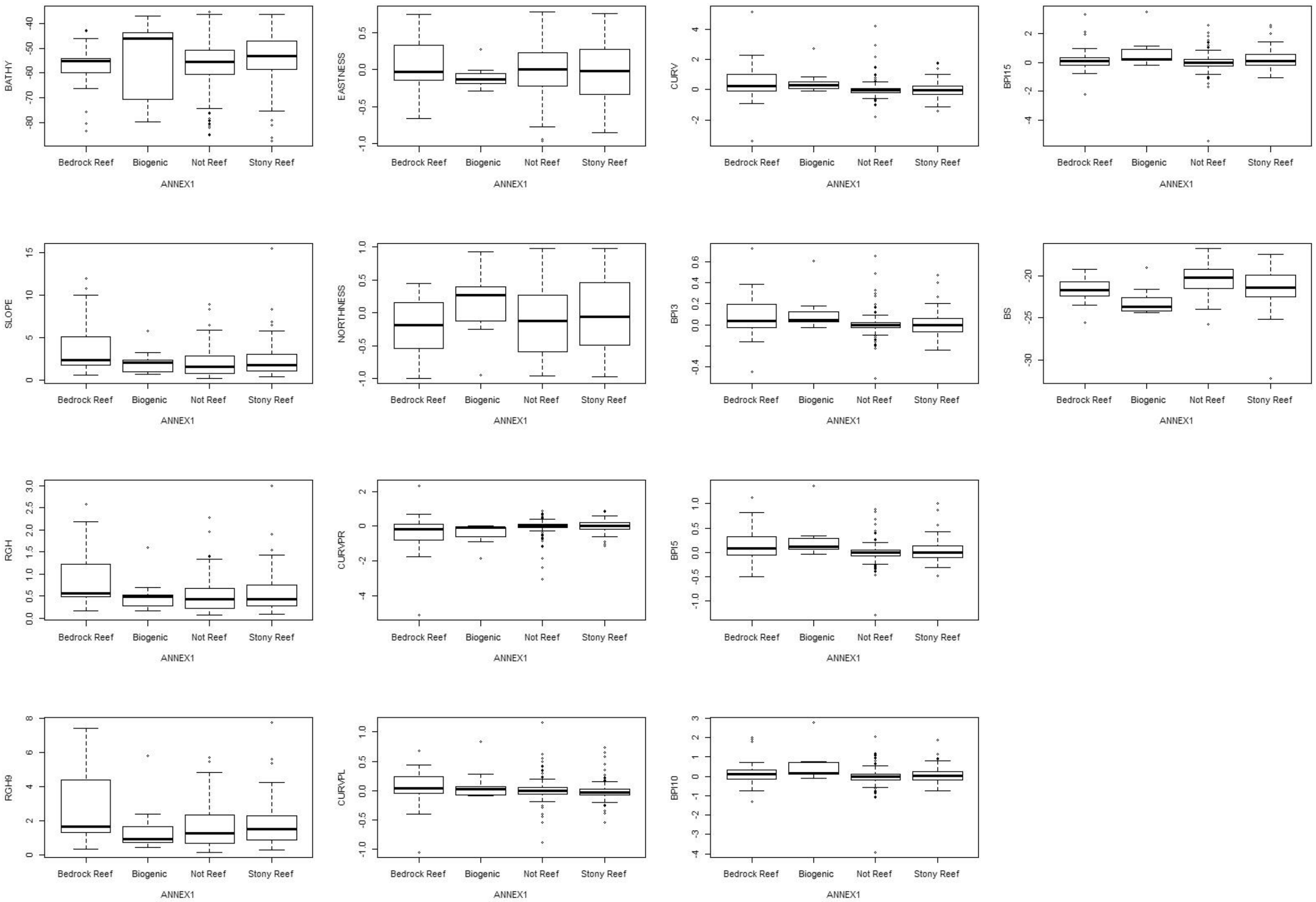

Figure 6. Box-plots showing mean (bold horizontal line), quartiles (boxes), 95% confidence intervals (whiskers) and outliers (asterisks) for the four categories bedrock reef, biogenic reef, not reef and stony reef and the different acoustic features bathymetry (BATHY), slope (SLOPE), roughness 3x3 (RGH), roughness 9x9 (RGH9), eastness (EASTNESS), northness (NORTHNESS), profile curvature (CURVPR), planar curvature (CURVPL), combined curvature (CURV), BPI3, BPI5, BPI10, BPI15 and backscatter (BS).

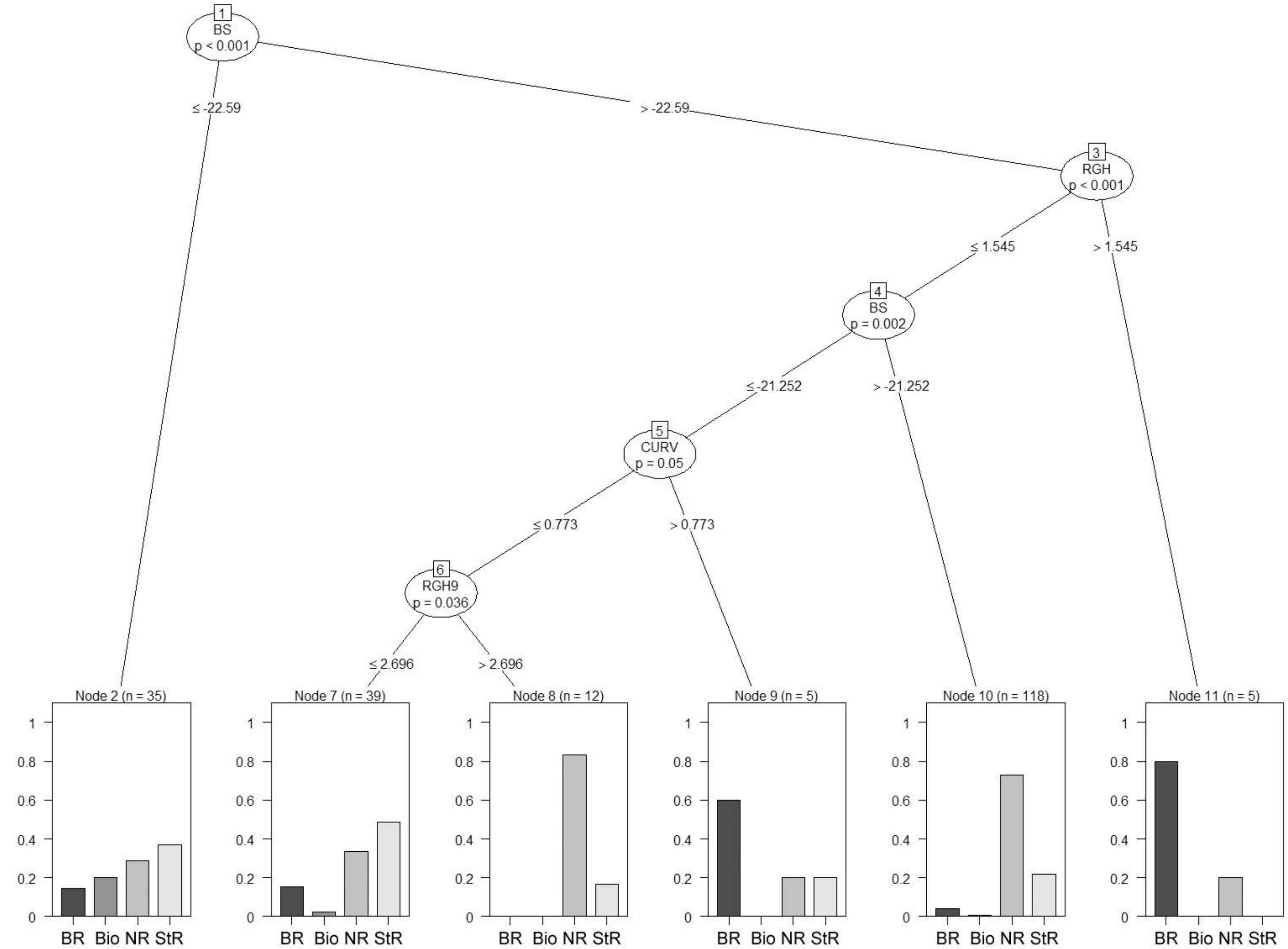

Figure 7. Conditional inference tree showing statistically significant splits in the acoustic features at nodes 1, 3, 4, 5 and 6. Terminal nodes 2, 7, 8, 9, 10 and 11 reveal a high degree of impurity. Key: BR – bedrock reef; Bio – biogenic reef; NR – not reef; StR – stony reef.

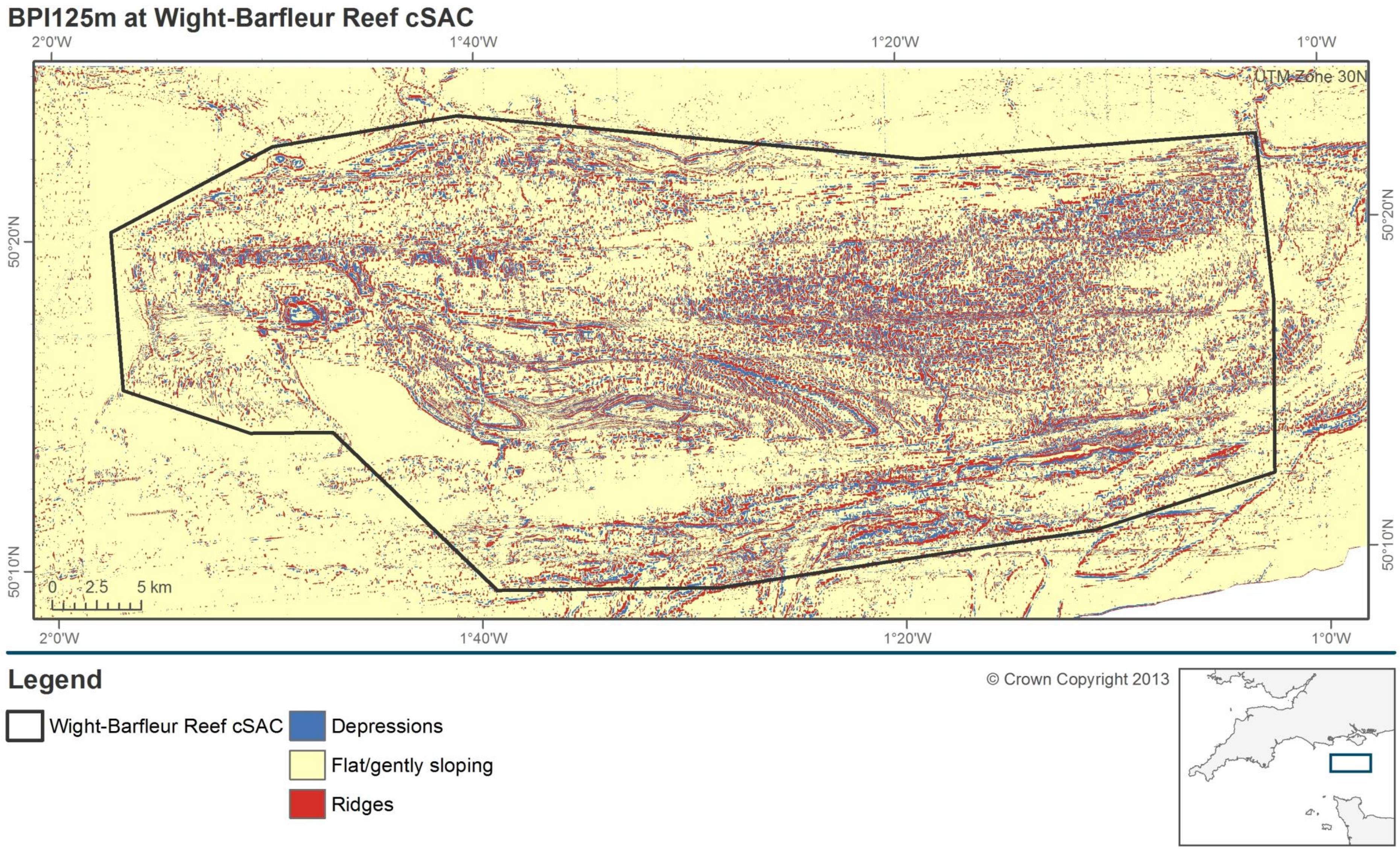

Figure 8. BPI with a neighbourhood size of 125m classified into depressions, flat or gently sloping seabed and ridges.

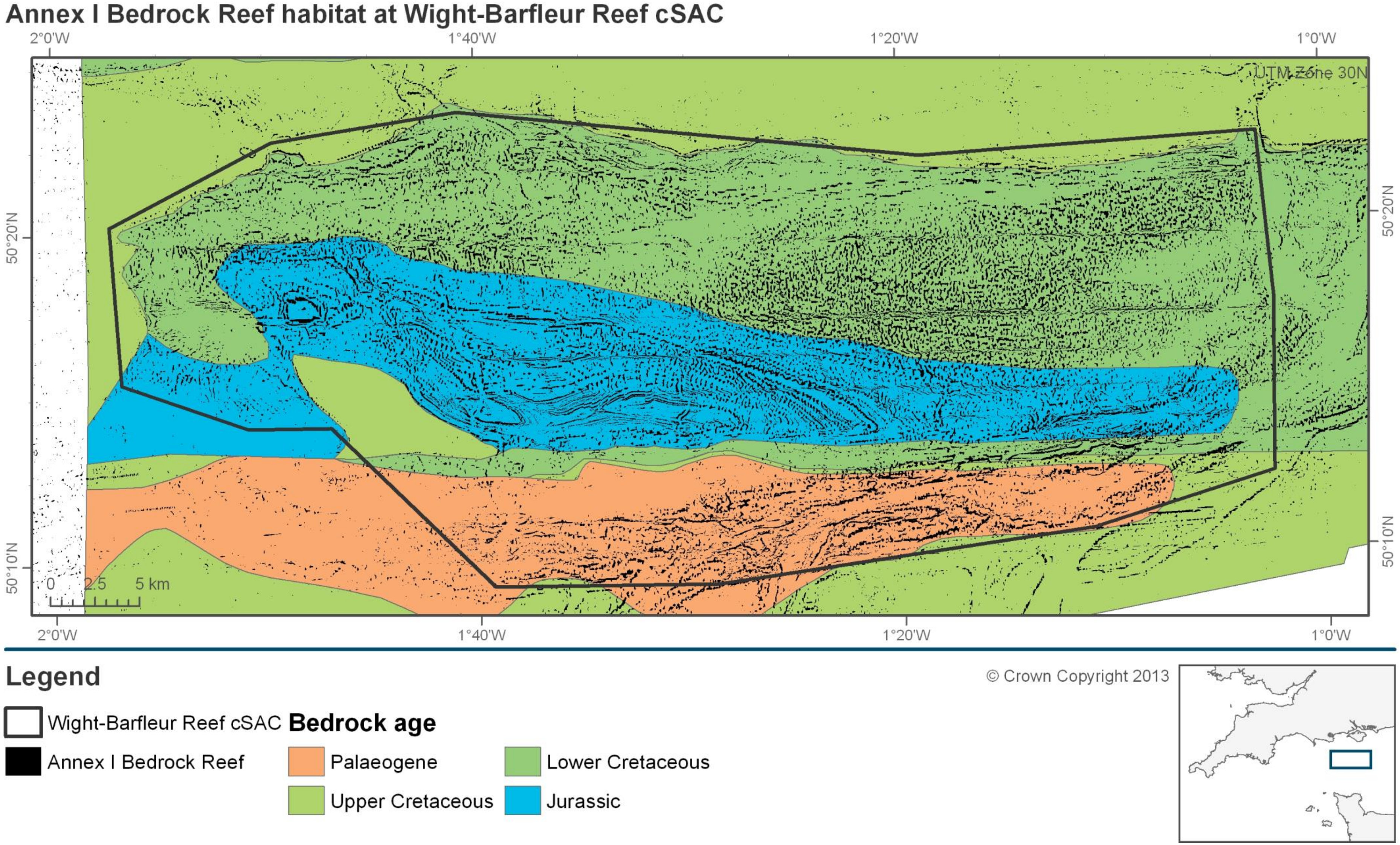

Figure 9. Distribution of Annex I bedrock reef at Wight-Barfleur Reef cSAC.

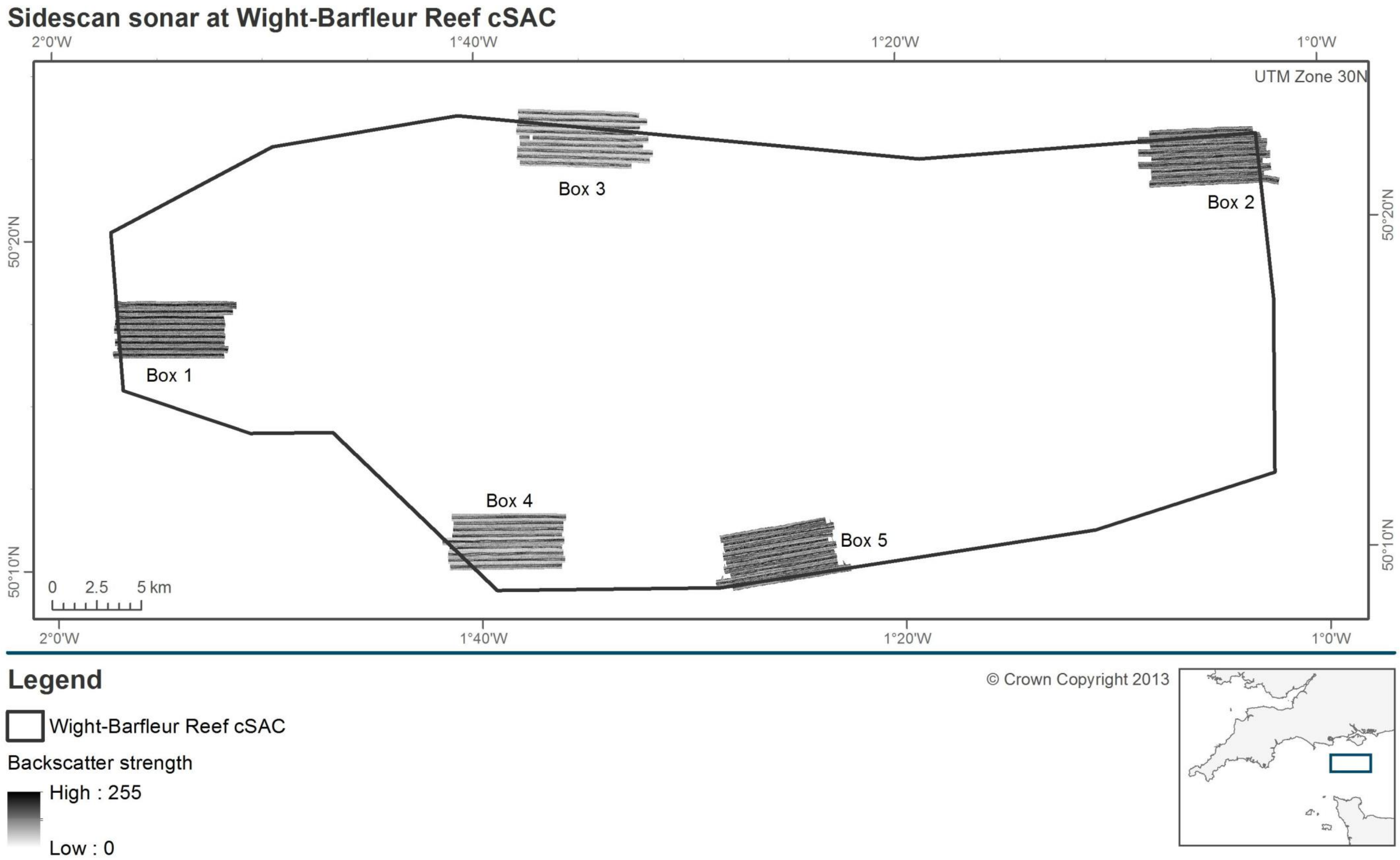

Figure 10. Overview of side-scan sonar data acquired at each of the five intensely surveyed boxes on the perimeter of the Wight-Barfleur Reef cSAC.

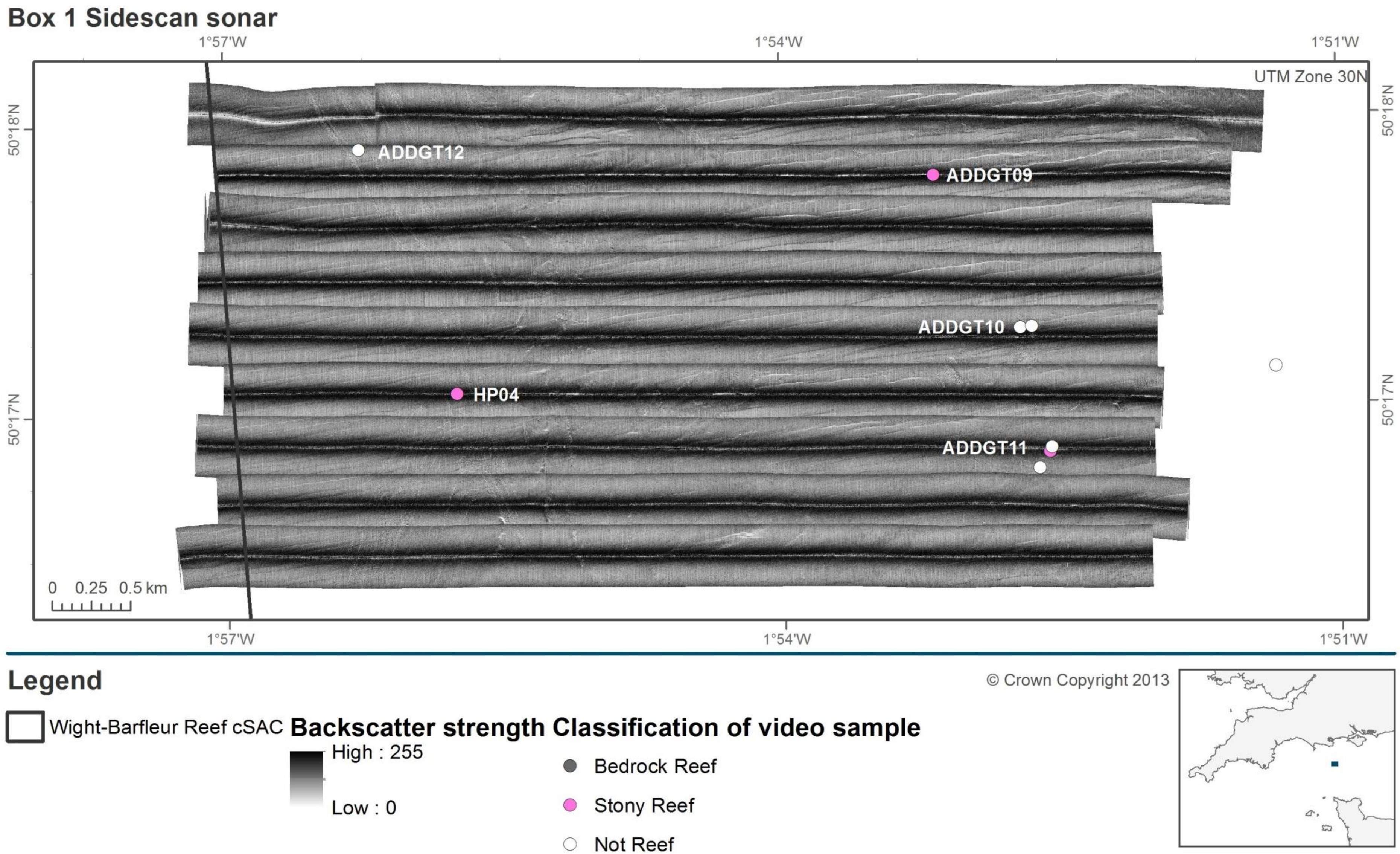

Figure 11. Overview of side-scan sonar acquired within Wight-Barfleur Reef cSAC Box 1.

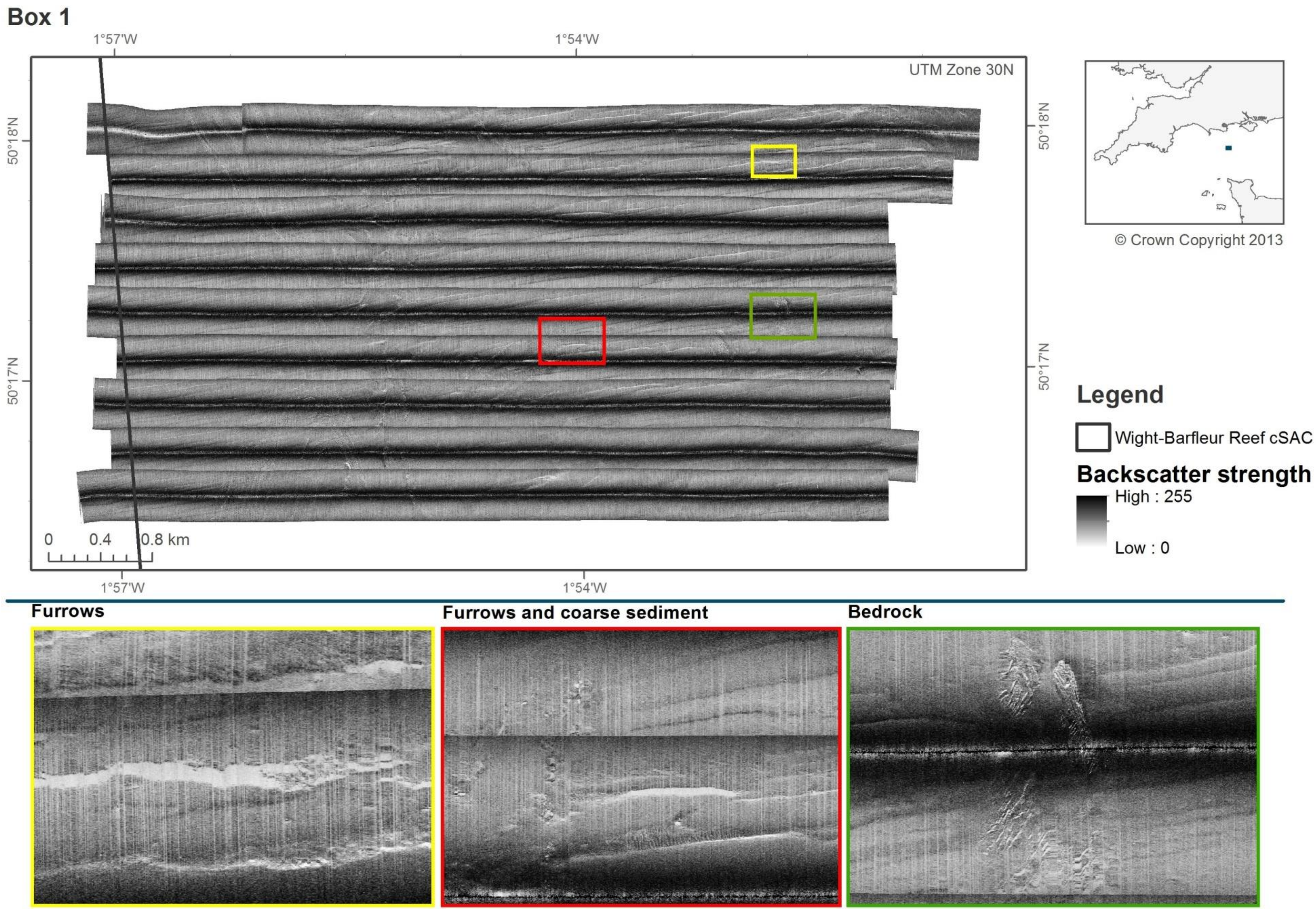

Figure 12. Examples of side-scan sonar signature type including bedrock, furrows and coarse sediment from Box 1 of Wight-Barfleur Reef cSAC.

Figure 13. Seabed substrate map based on the acoustic and ground-truthing data from Wight-Barfleur Reef cSAC Box 1.

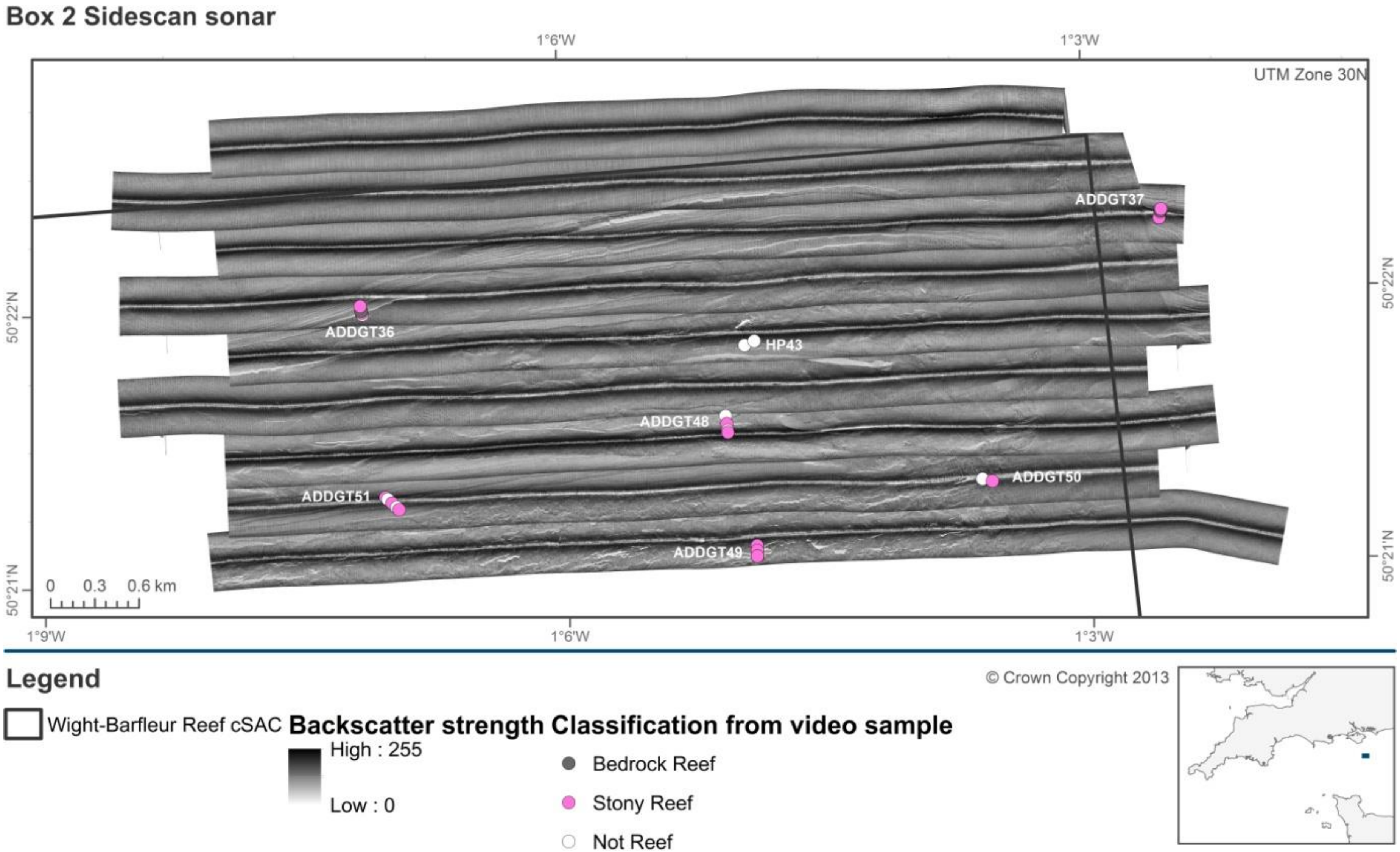

Figure 14. Overview of side-scan sonar acquired within Wight-Barfleur Reef cSAC Box 2.

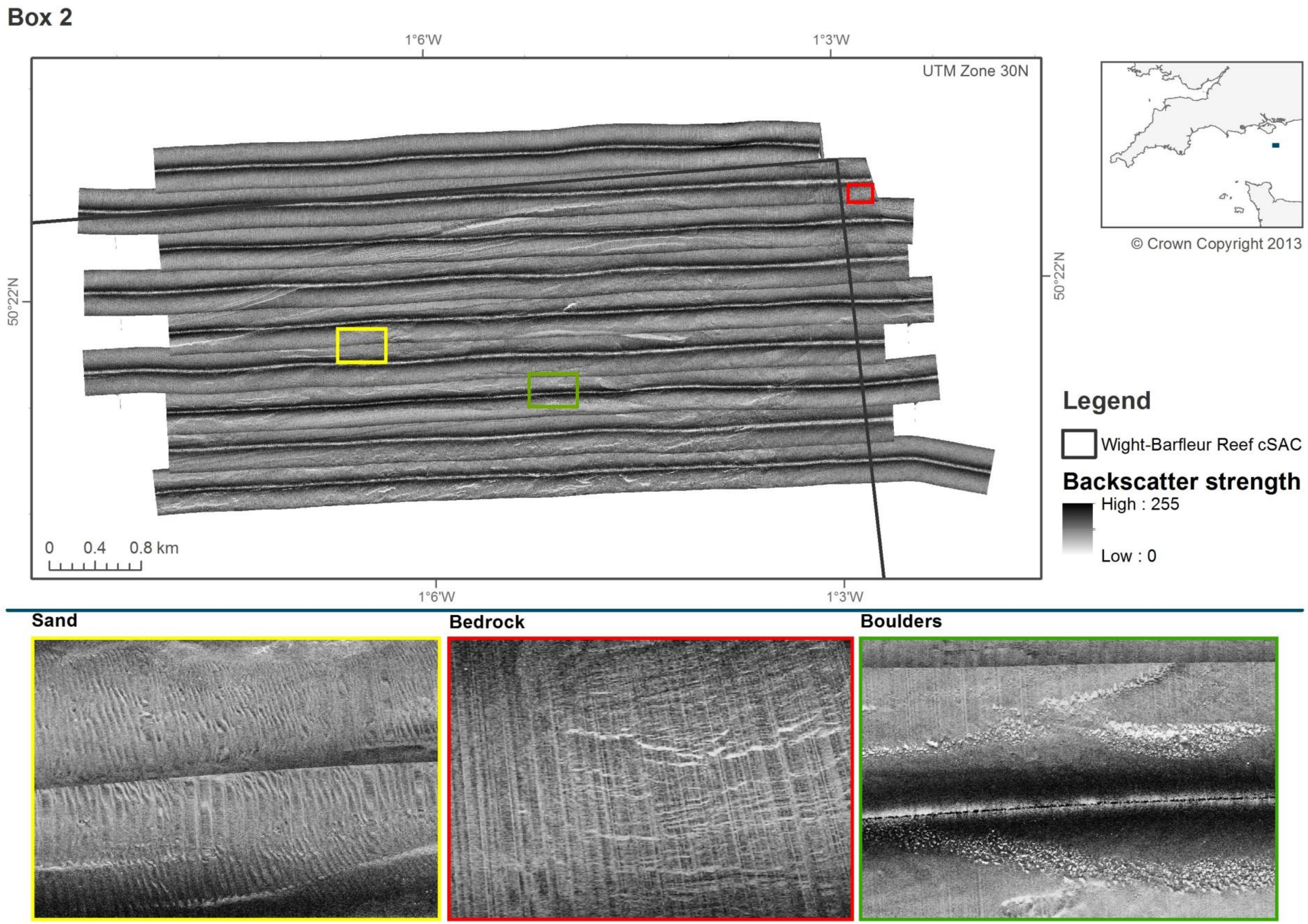

Figure 15. Examples of side-scan sonar signature type including sand, bedrock and boulders from Box 2 of Wight-Barfleur Reef cSAC.

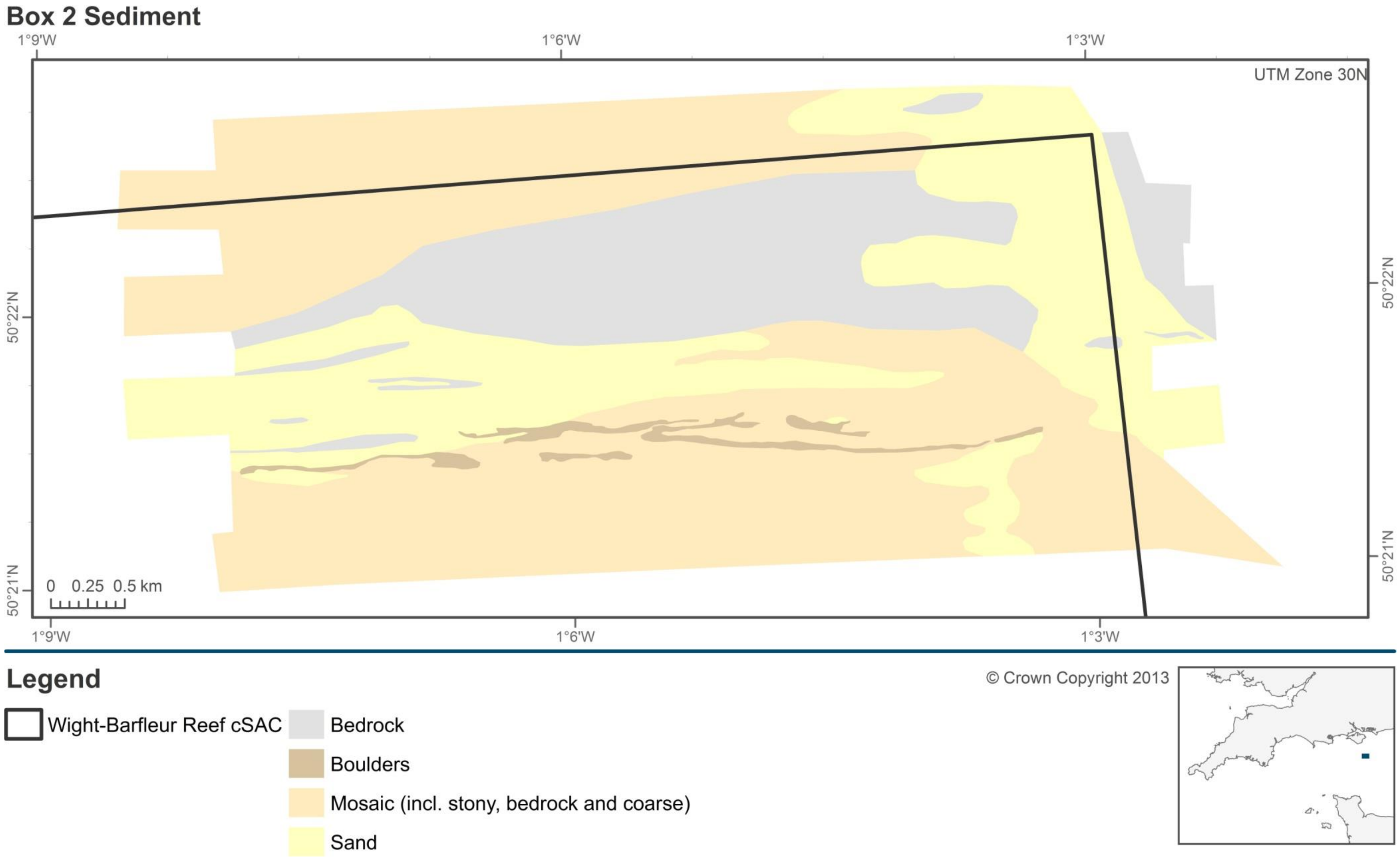

Figure 16. Seabed substrate map based on the acoustic and ground-truthing data from Wight-Barfleur Reef cSAC Box 2.

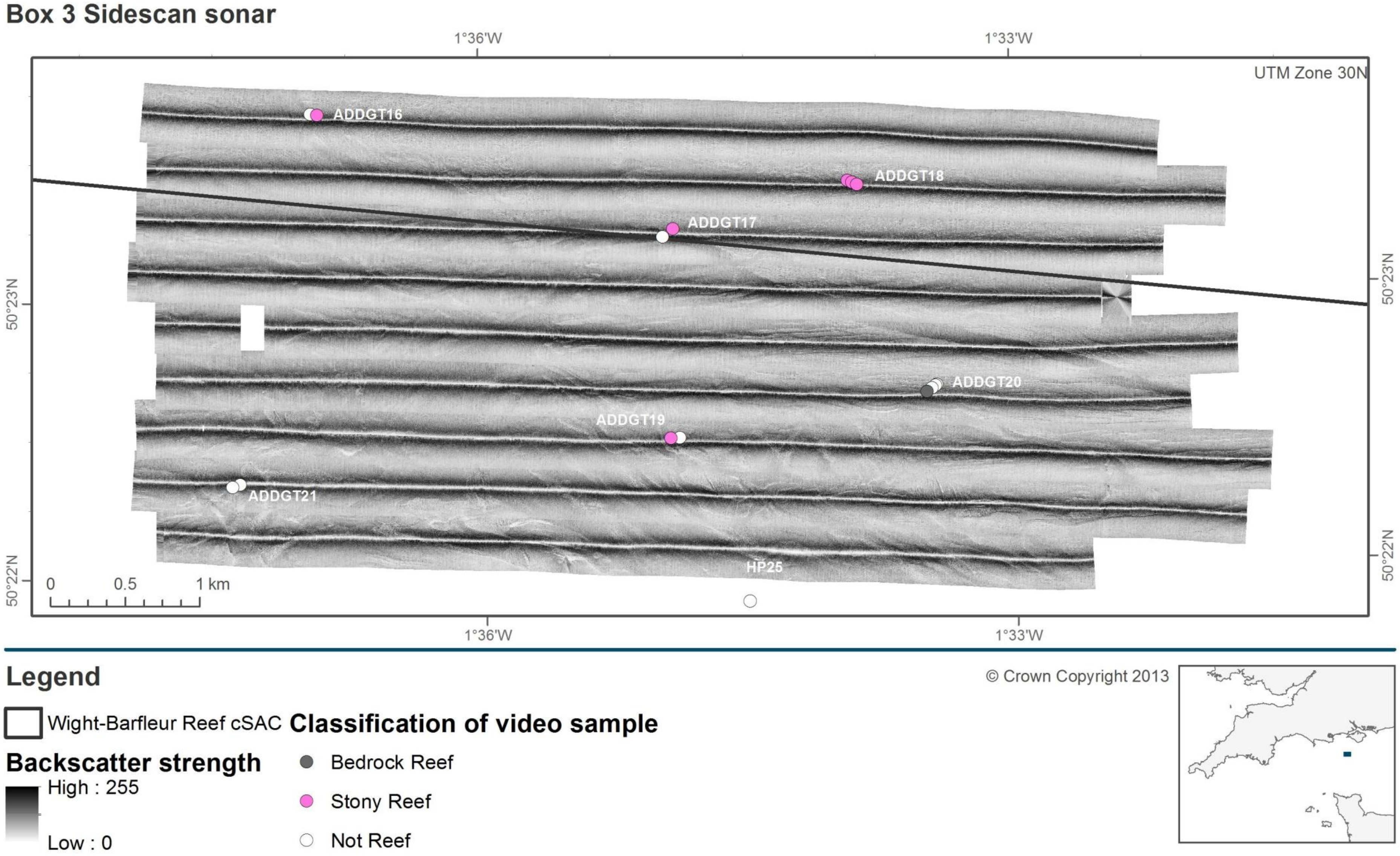

Figure 17. Overview of side-scan sonar acquired within Wight-Barfleur Reef cSAC Box 3.

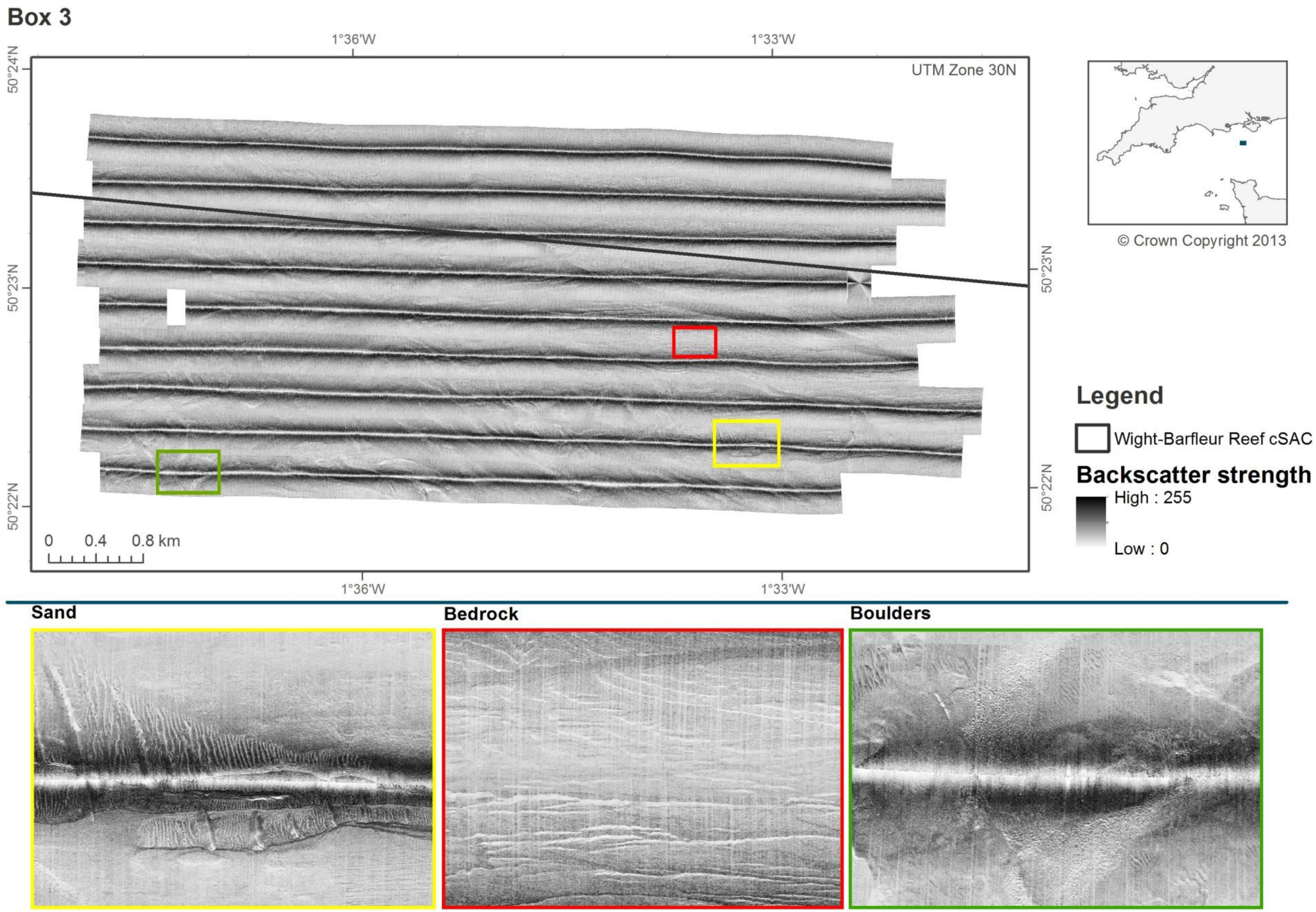

Figure 18. Examples of side-scan sonar signature type including sand, bedrock and boulders from Box 3 of Wight-Barfleur Reef cSAC.

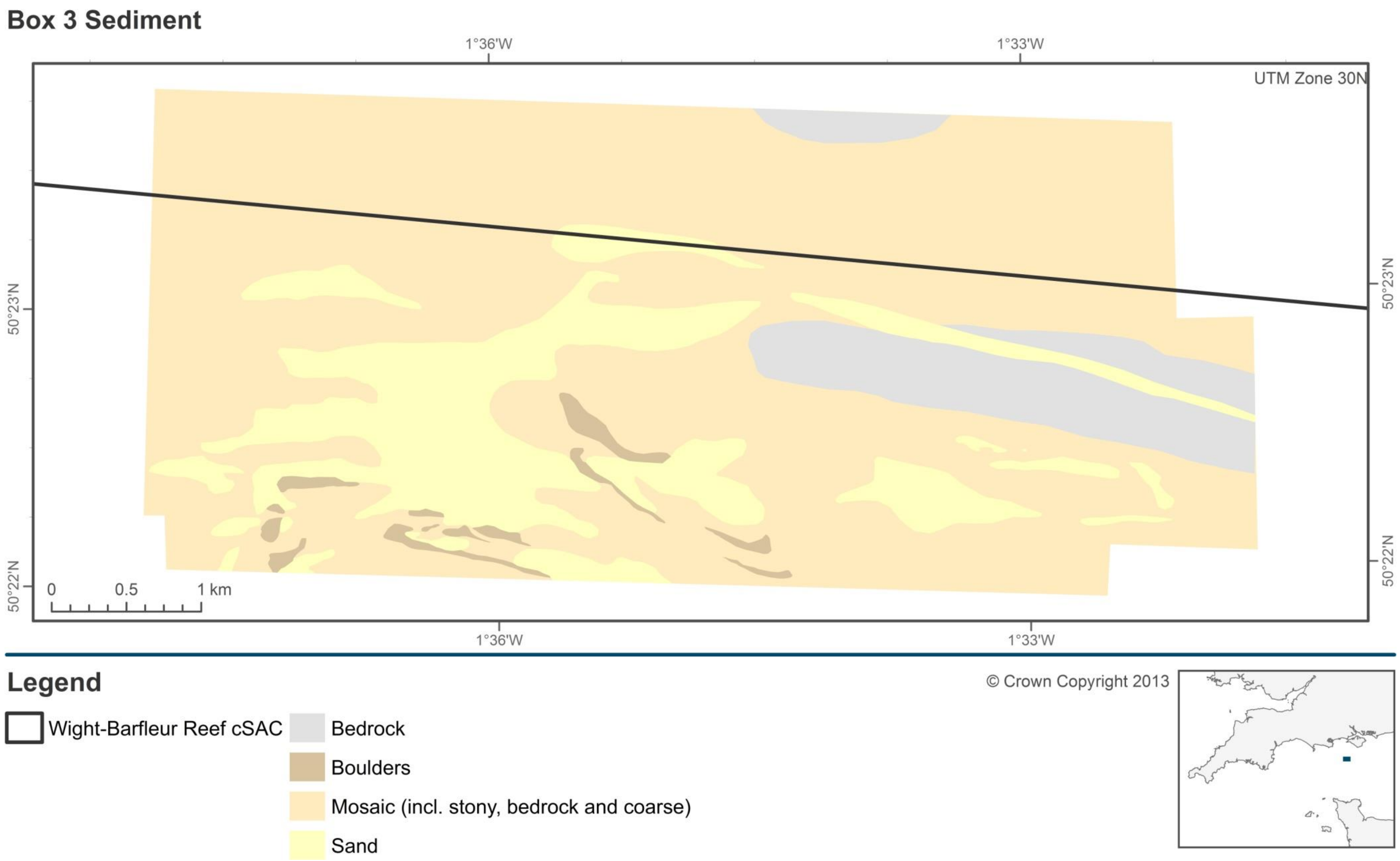

Figure 19. Seabed substrate map based on the acoustic and ground-truthing data from Wight-Barfleur Reef cSAC Box 3.

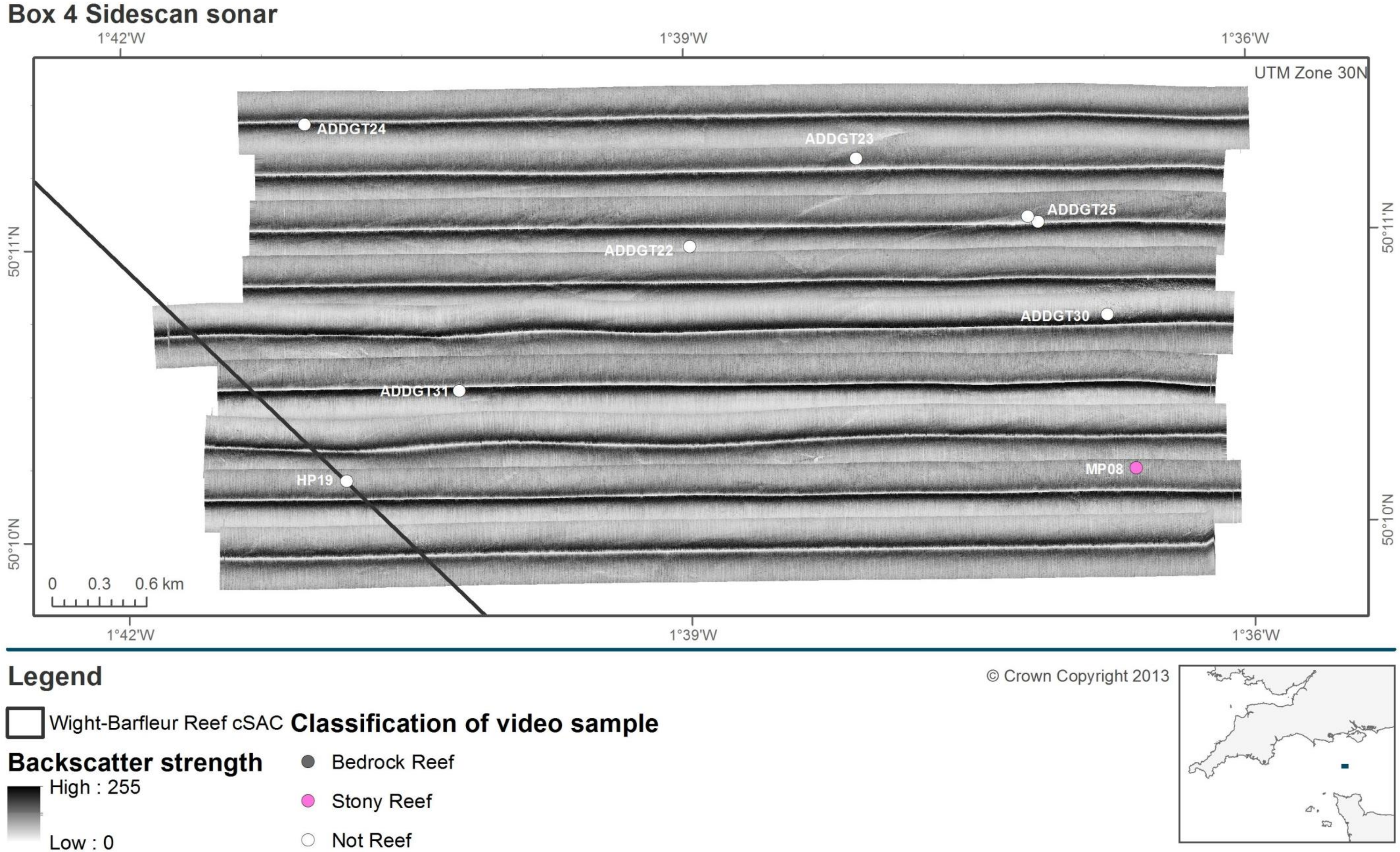

Figure 20. Overview of side-scan sonar acquired within Wight-Barfleur Reef cSAC Box 4.

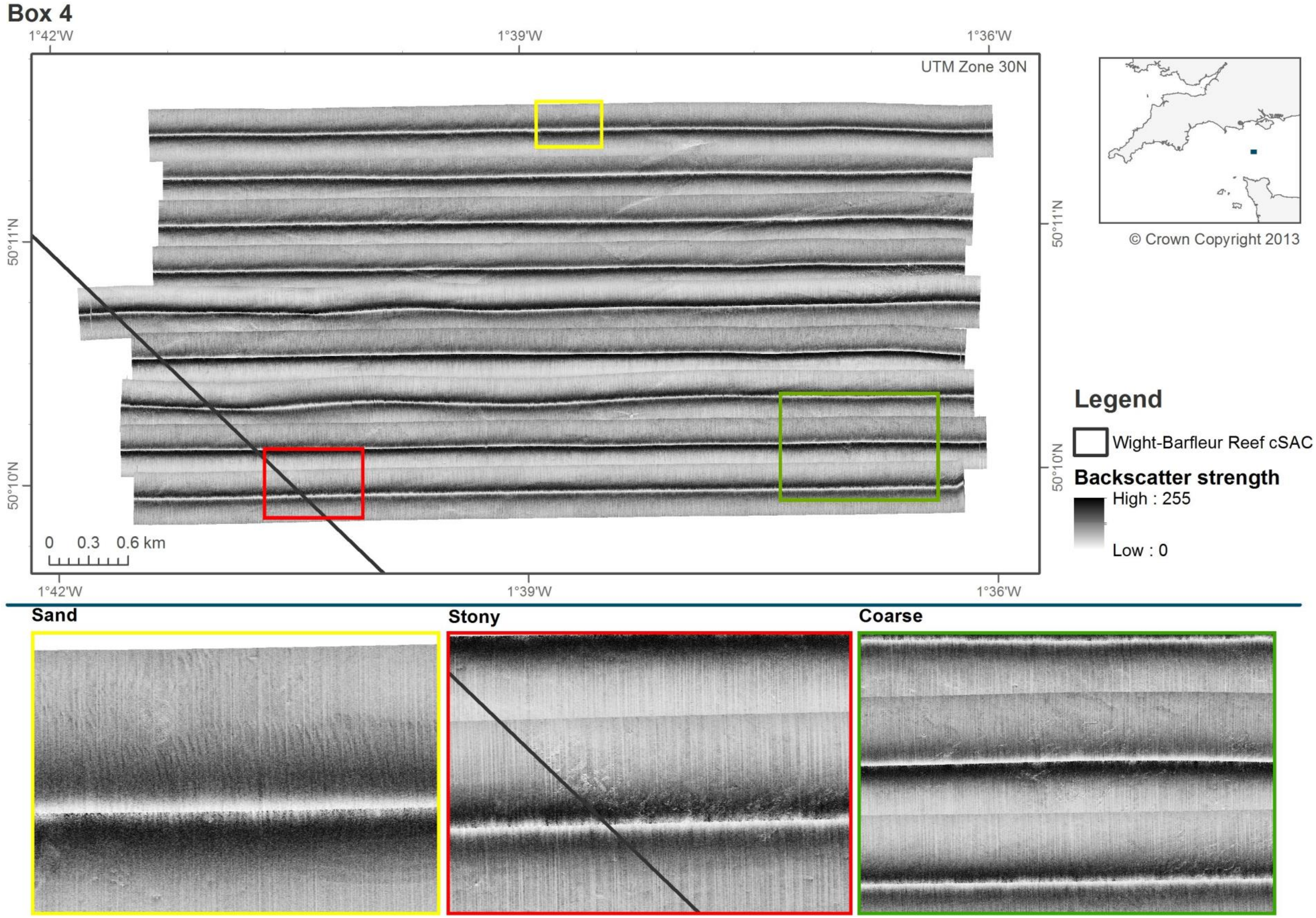

Figure 21. Examples of side-scan sonar signature type including sand, stony and coarse from Box 4 of Wight-Barfleur Reef cSAC.

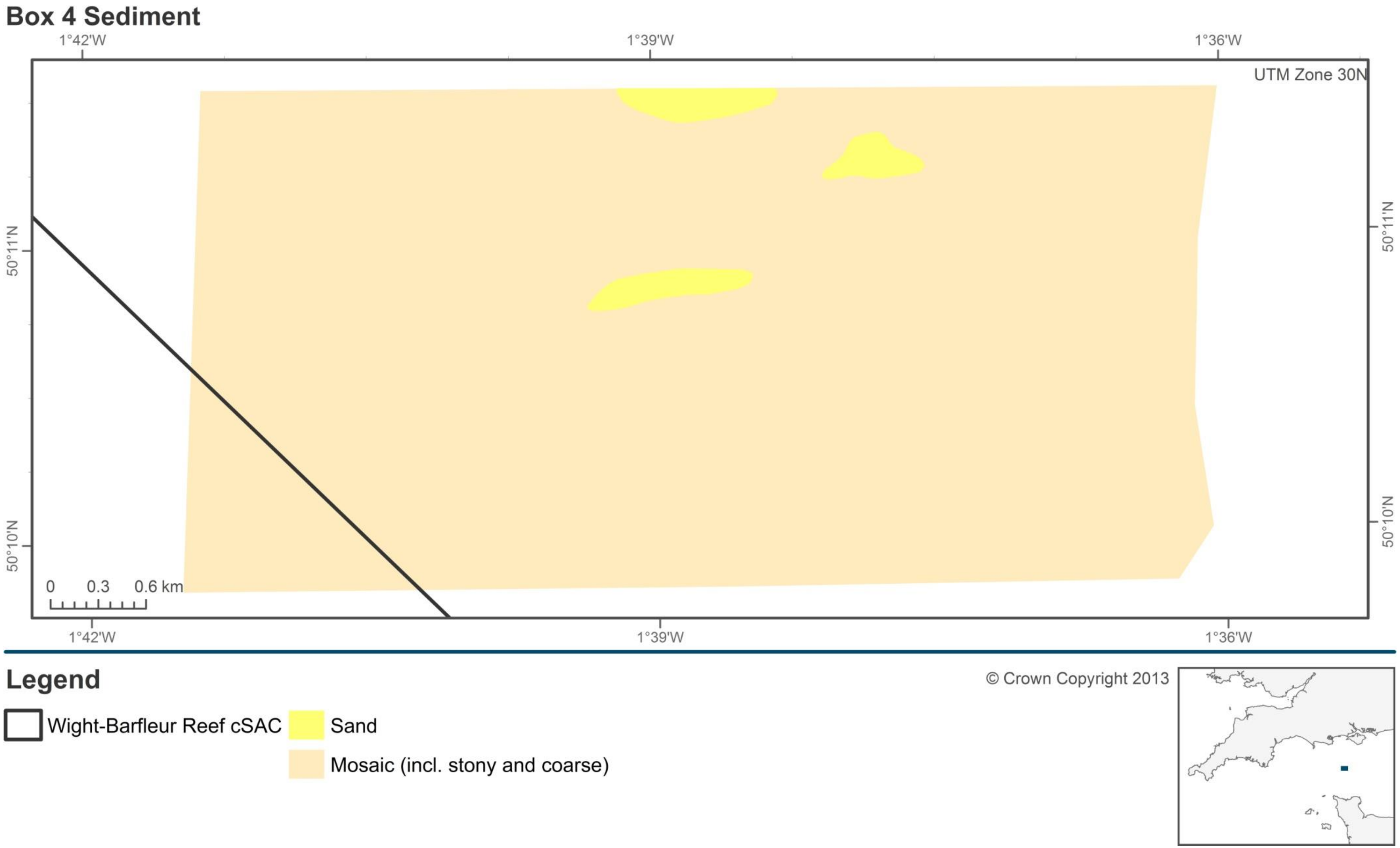

Figure 22. Seabed substrate map based on the acoustic and ground-truthing data from Wight-Barfleur Reef cSAC Box 4.

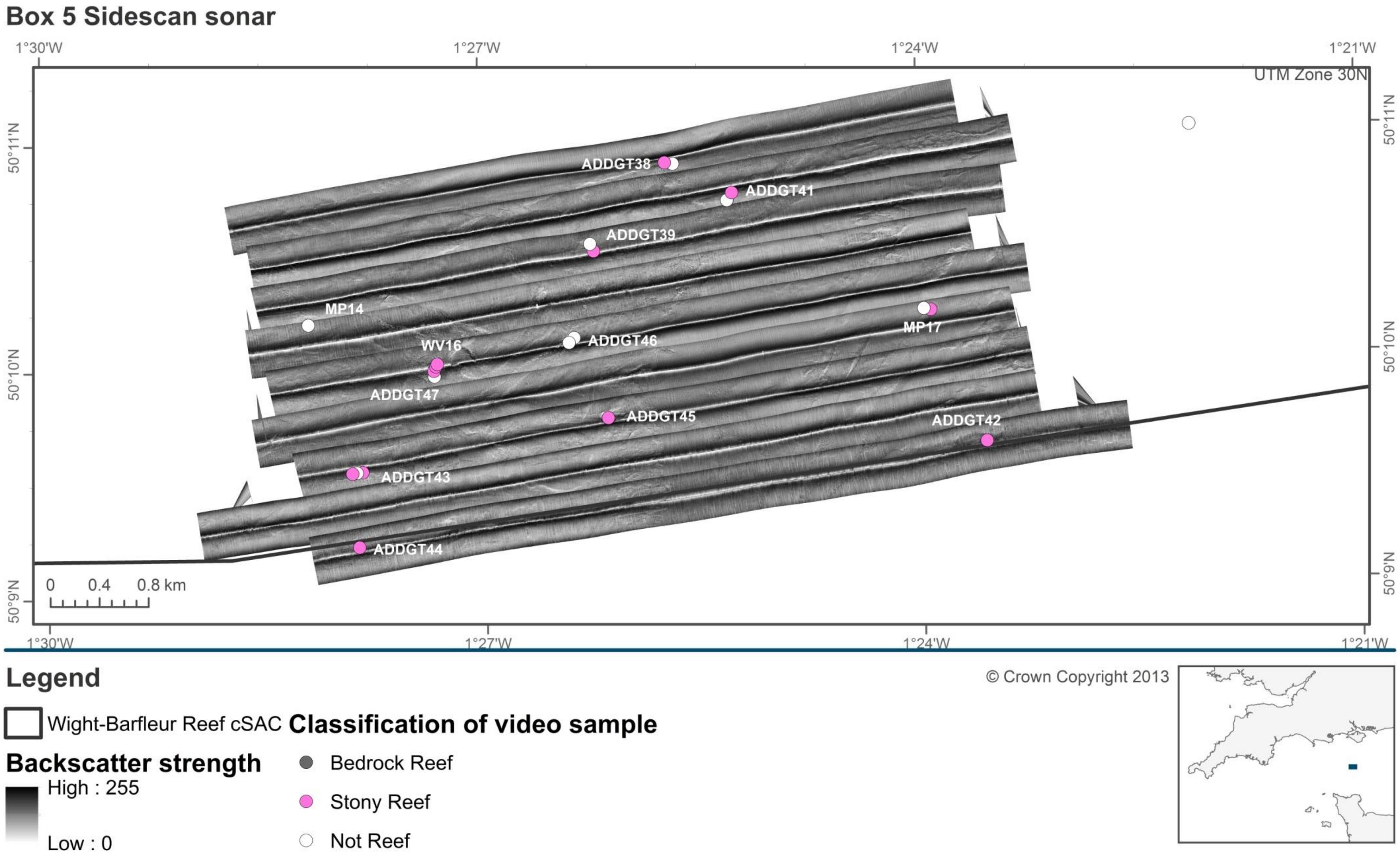

Figure 23. Overview of side-scan sonar acquired within Wight-Barfleur Reef cSAC Box 5.

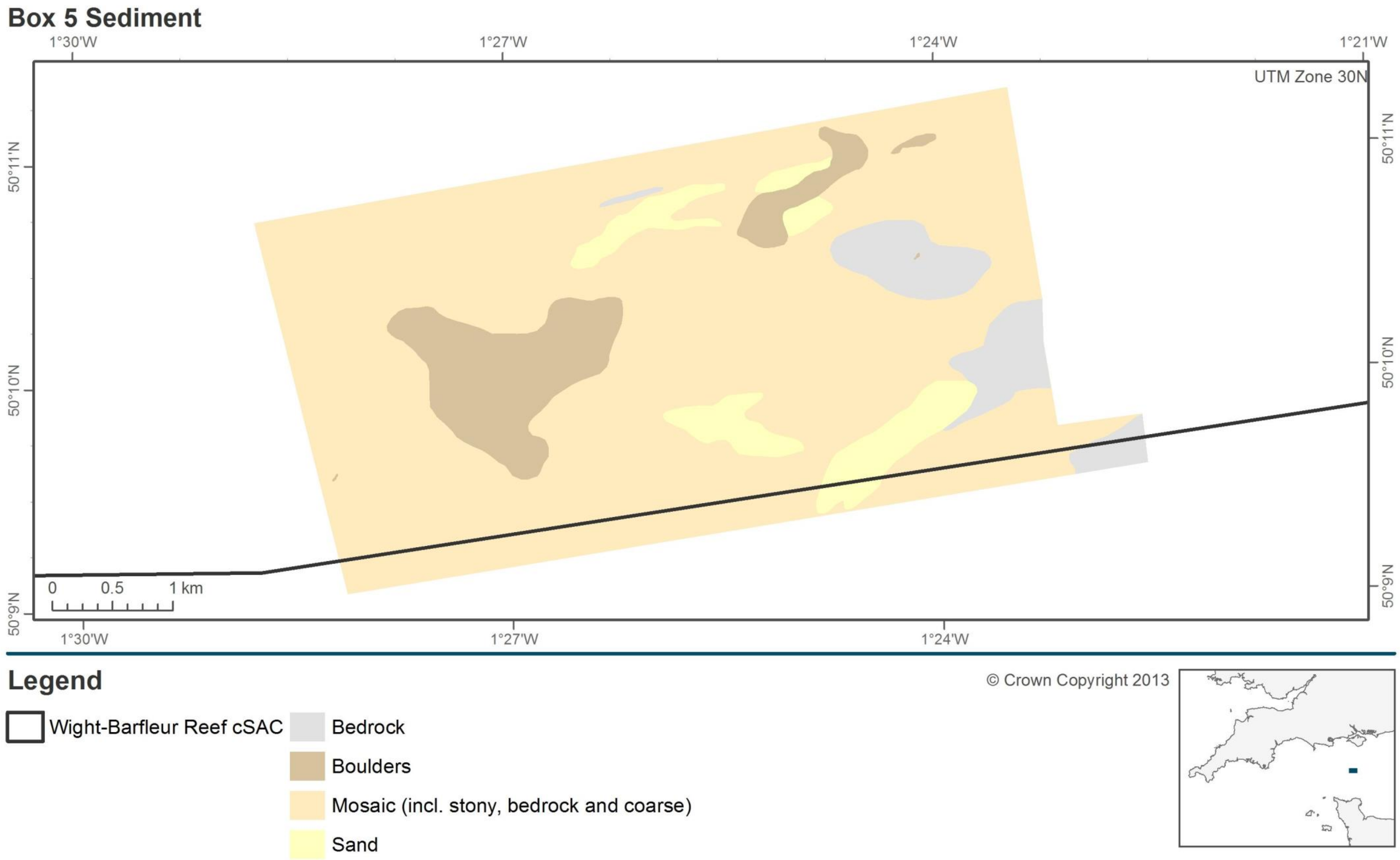

Figure 24. Seabed substrate map based on the acoustic and ground-truthing data from Wight-Barfleur Reef cSAC Box 5.

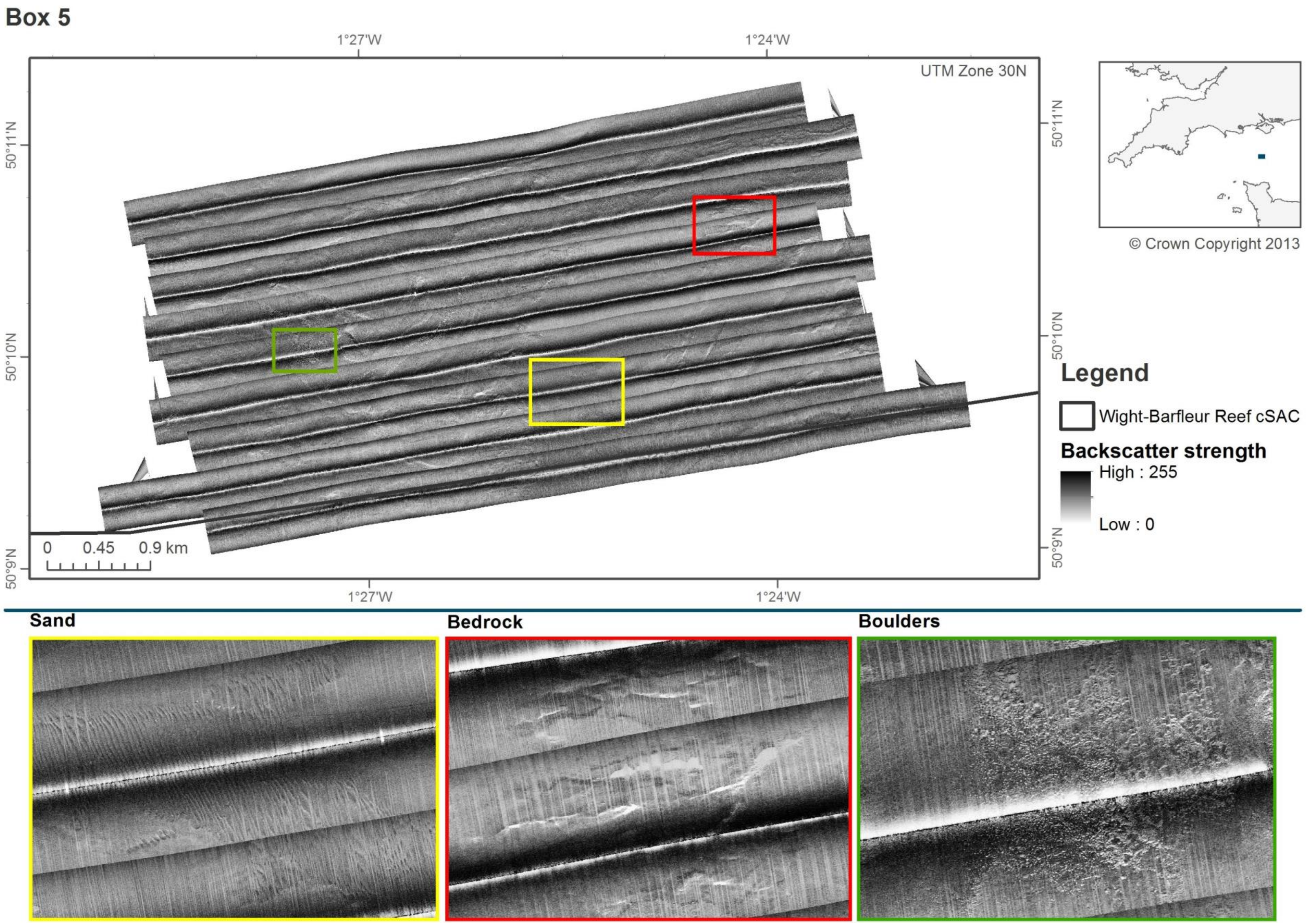

Figure 25. Examples of side-scan sonar signature type including sand, bedrock and boulders from Box 5 of Wight-Barfleur Reef cSAC.

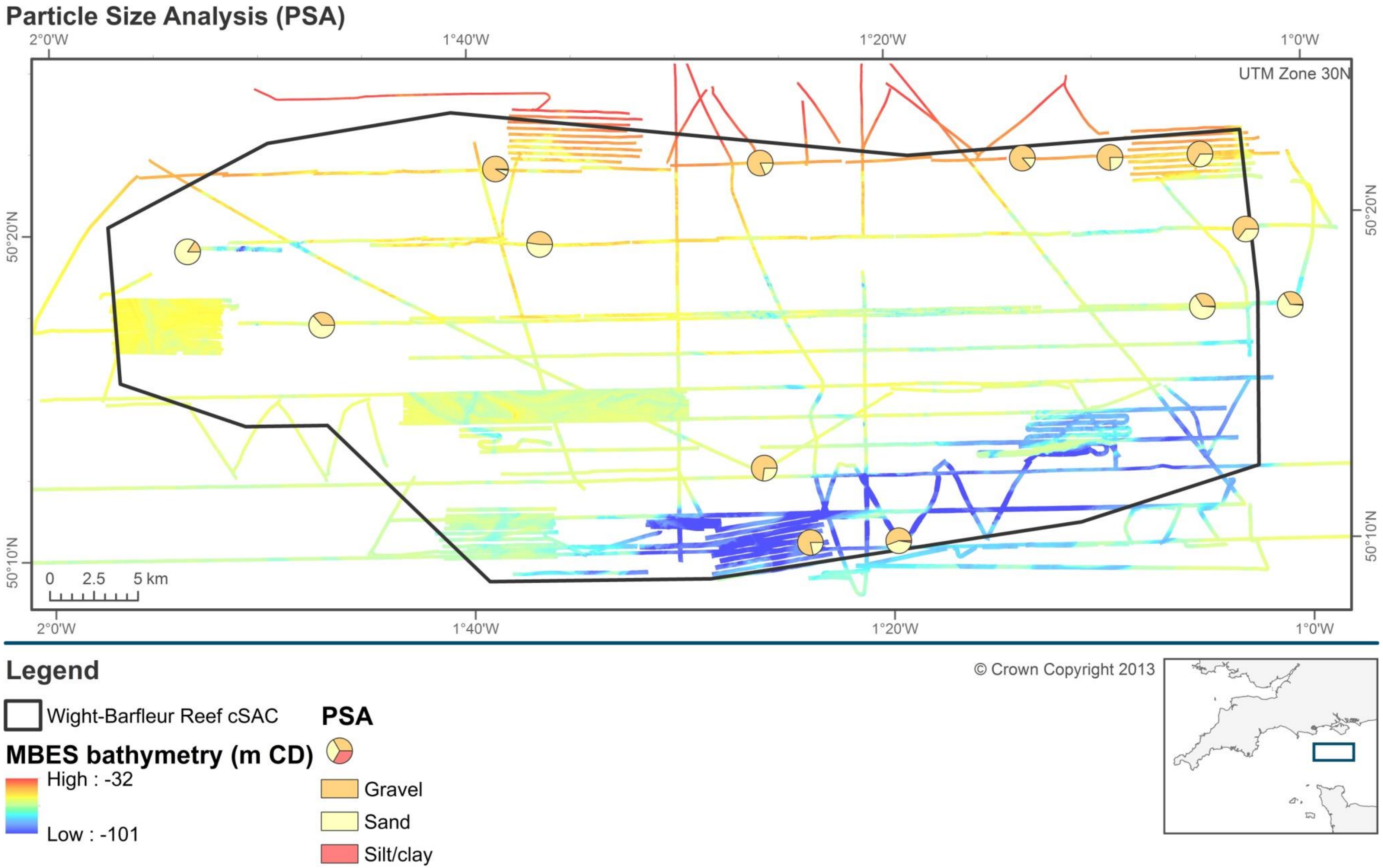

Figure 26. Breakdown of the different broad sediment classes within each sediment sample collected.

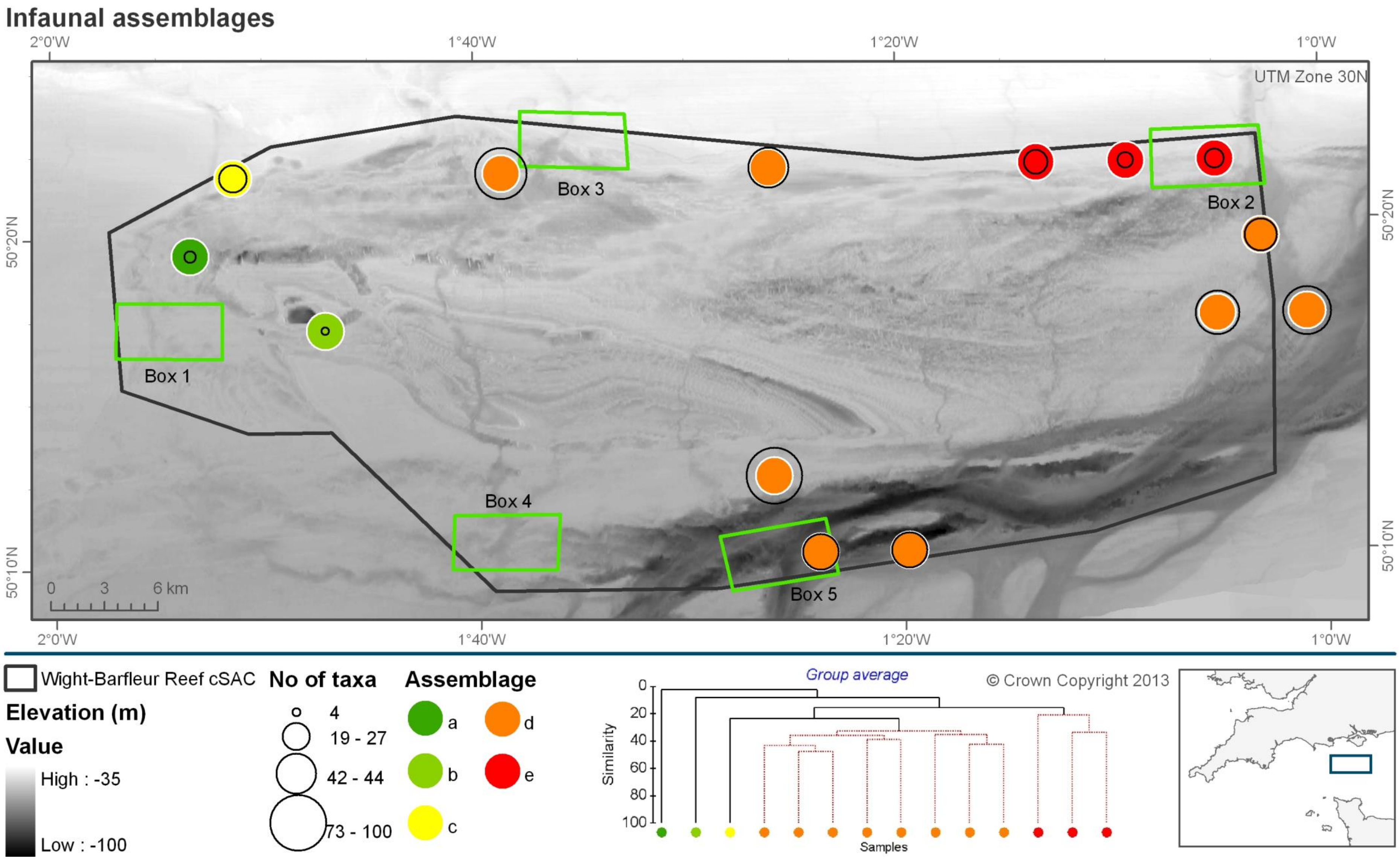

Figure 27. Distribution of distinct infaunal assemblages identified through multivariate analysis of square-root transformed taxon abundance data. Hollow circles are indicative of the number of taxa observed at each sampling station.

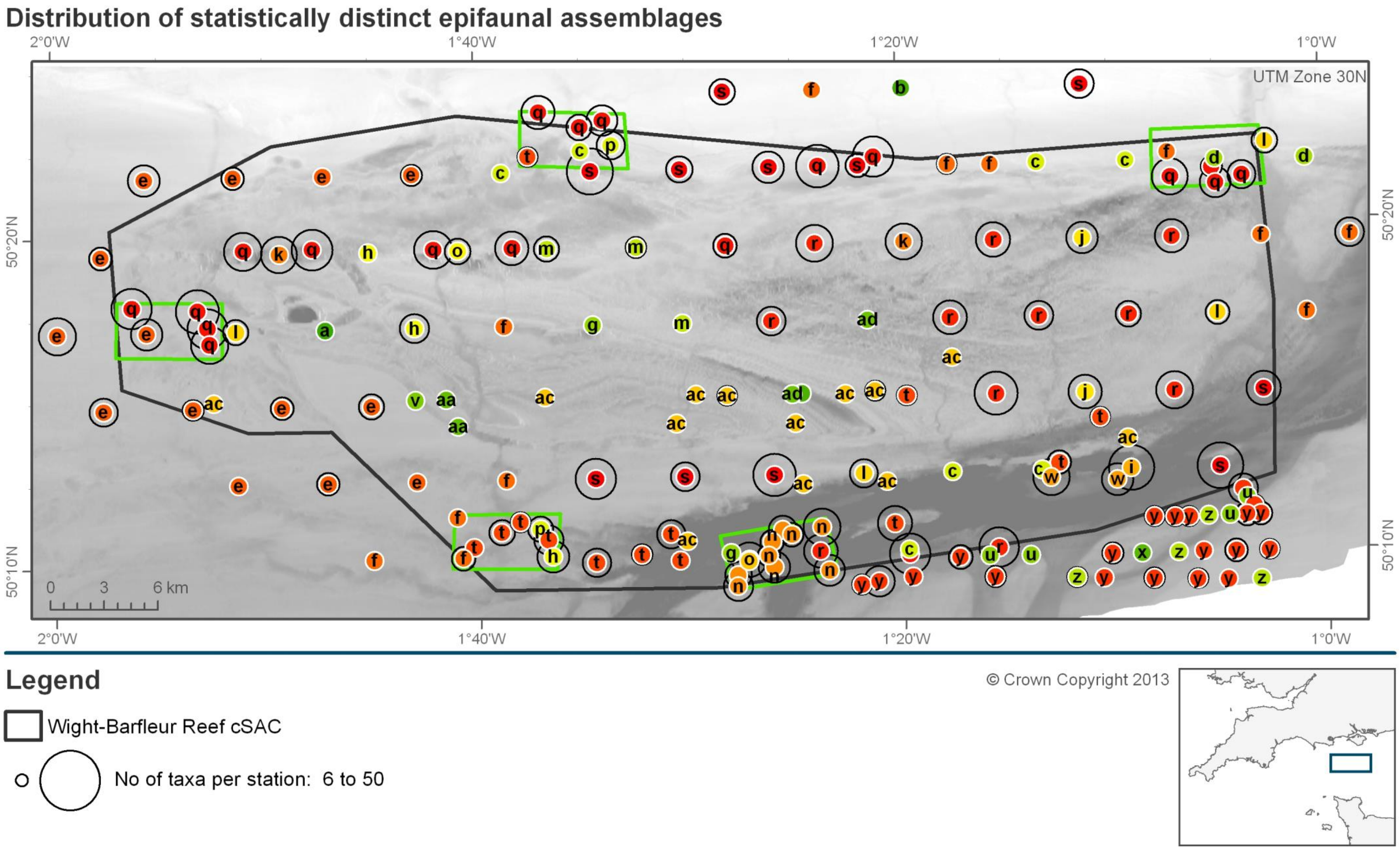

Figure 28. Distribution of statistically distinct assemblages identified through multivariate analysis. Each distinct assemblage (labelled a to z and aa to ad thereafter) is represented by a different shade from red to yellow to green in decreasing order of taxon richness. Black circles around each station are indicative of the total number of taxa recorded at each station.

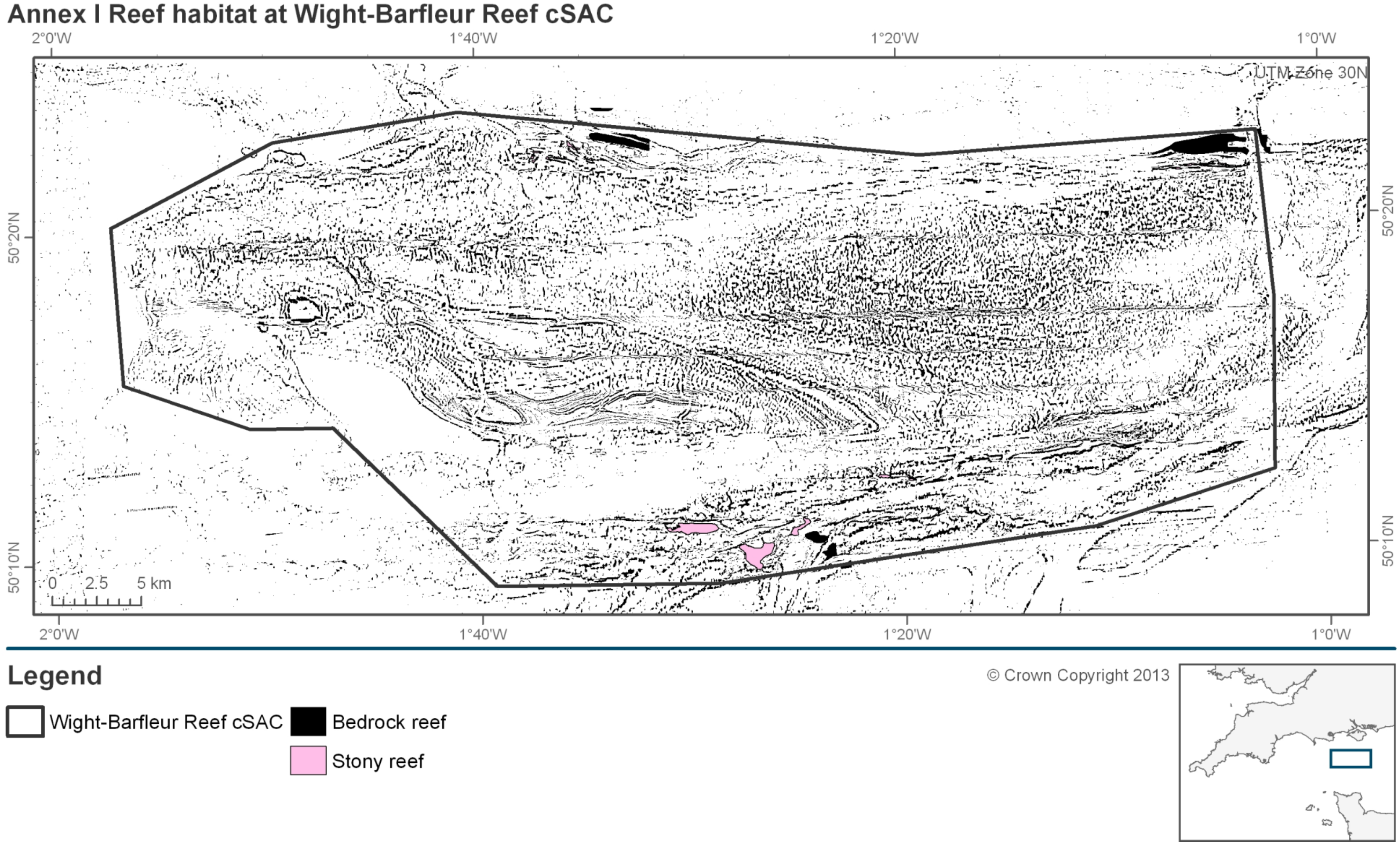

Figure 29. Distribution of Annex I Reef habitat, consisting of bedrock and stony substrate types.

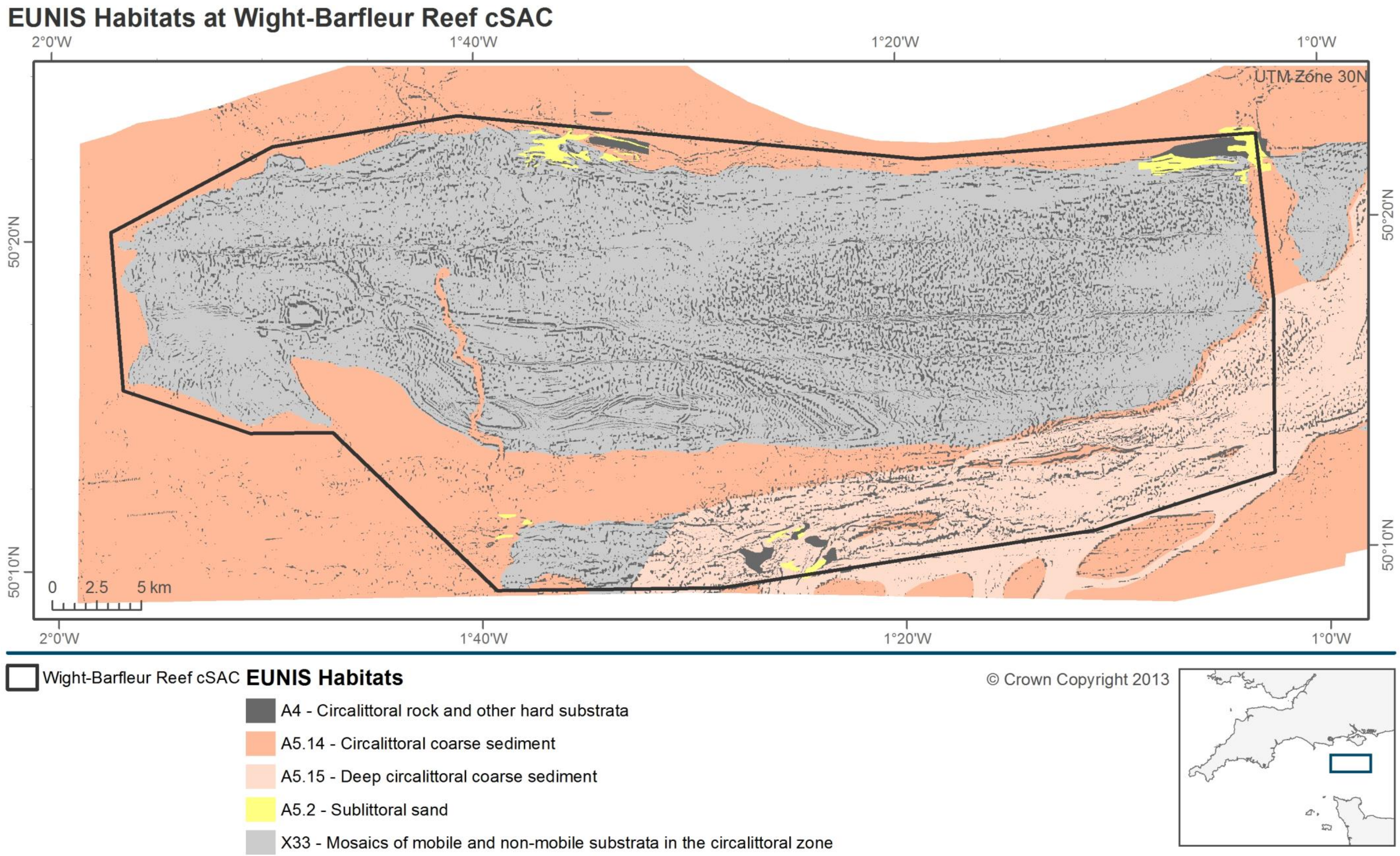

Figure 30. Updated EUNIS map for the area in and around the Wight-Barfleur Reef cSAC.

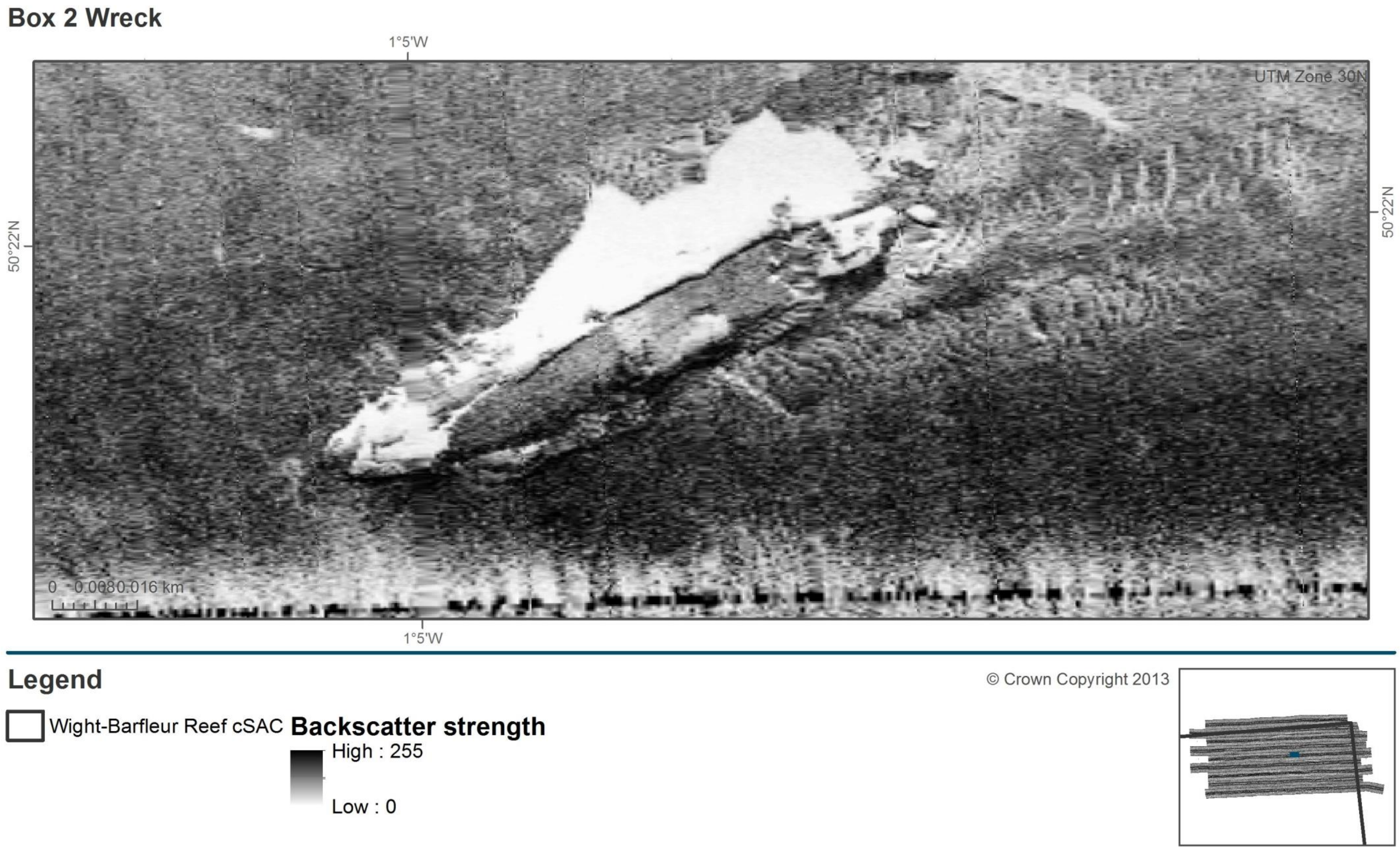

Figure 31. Detail of side-scan sonar record illustrating outline of a wreck on the seabed in Box 2.

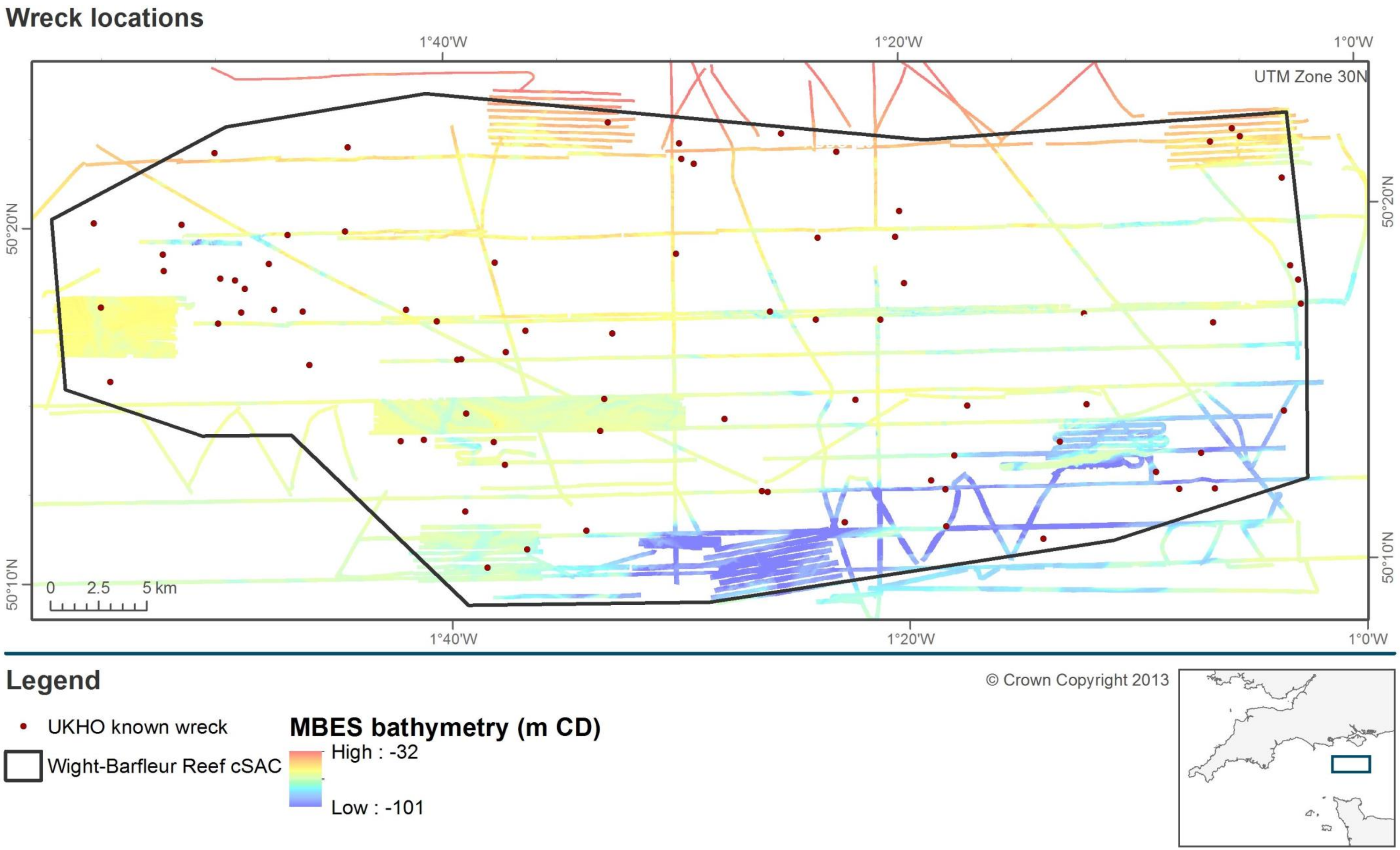

Figure 32. Location of known wrecks within the Wight-Barfleur Reef cSAC. Source: UKHO wreck database.

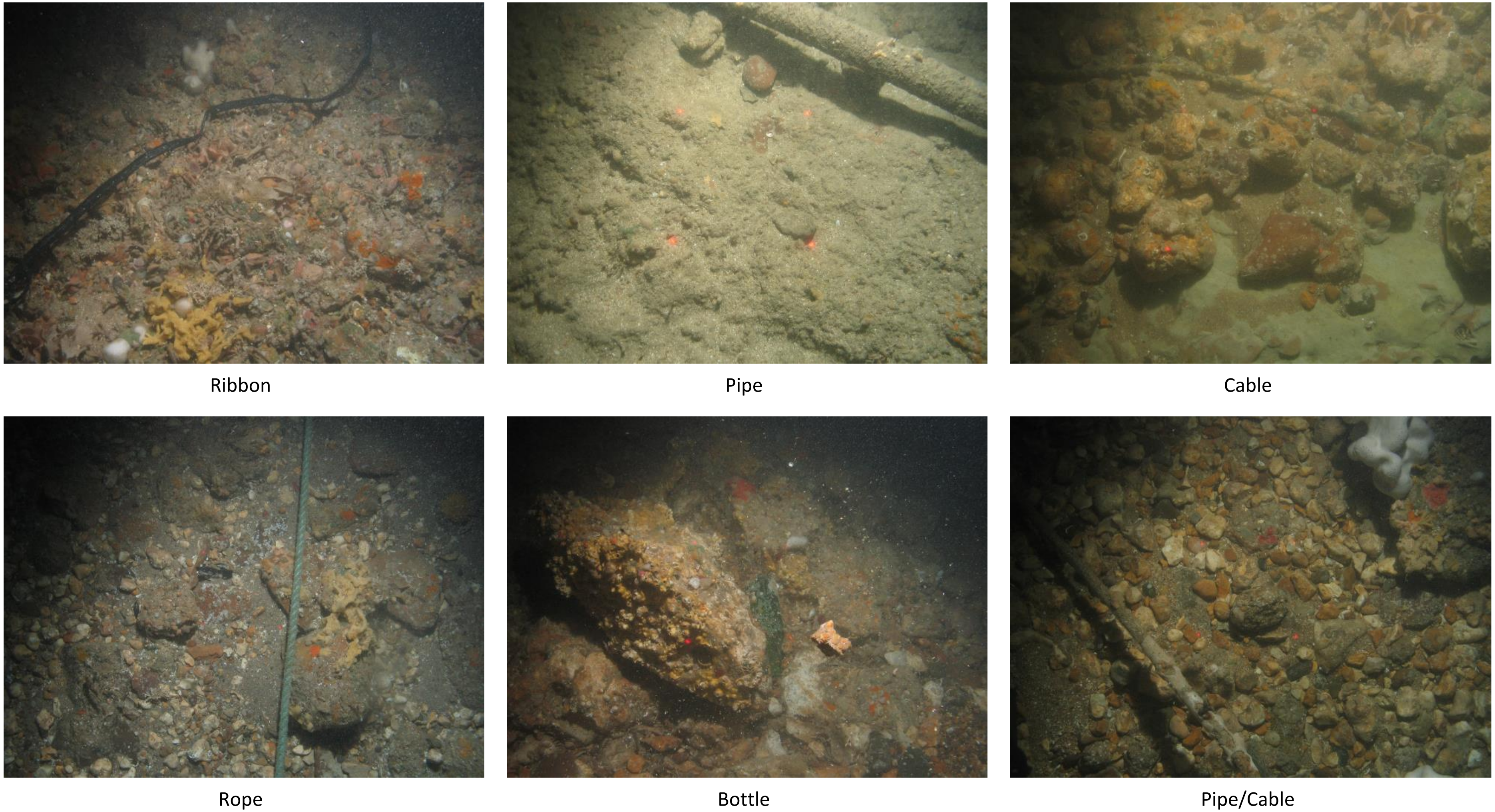

Figure 33. Evidence of marine litter on the seabed within the Wight Barfleur Reef cSAC.

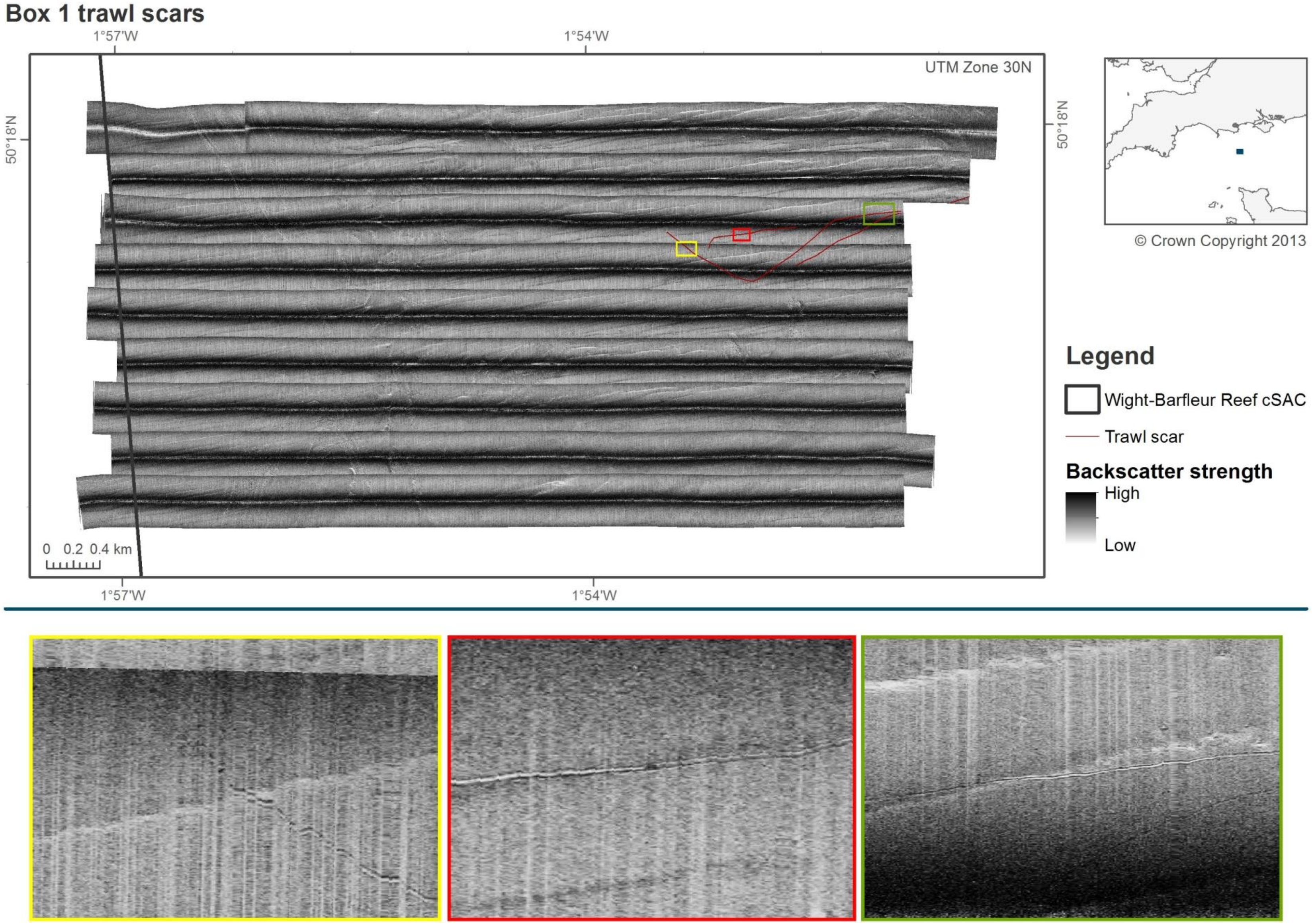

Figure 34. Trawl scars on the seabed at Box 1.

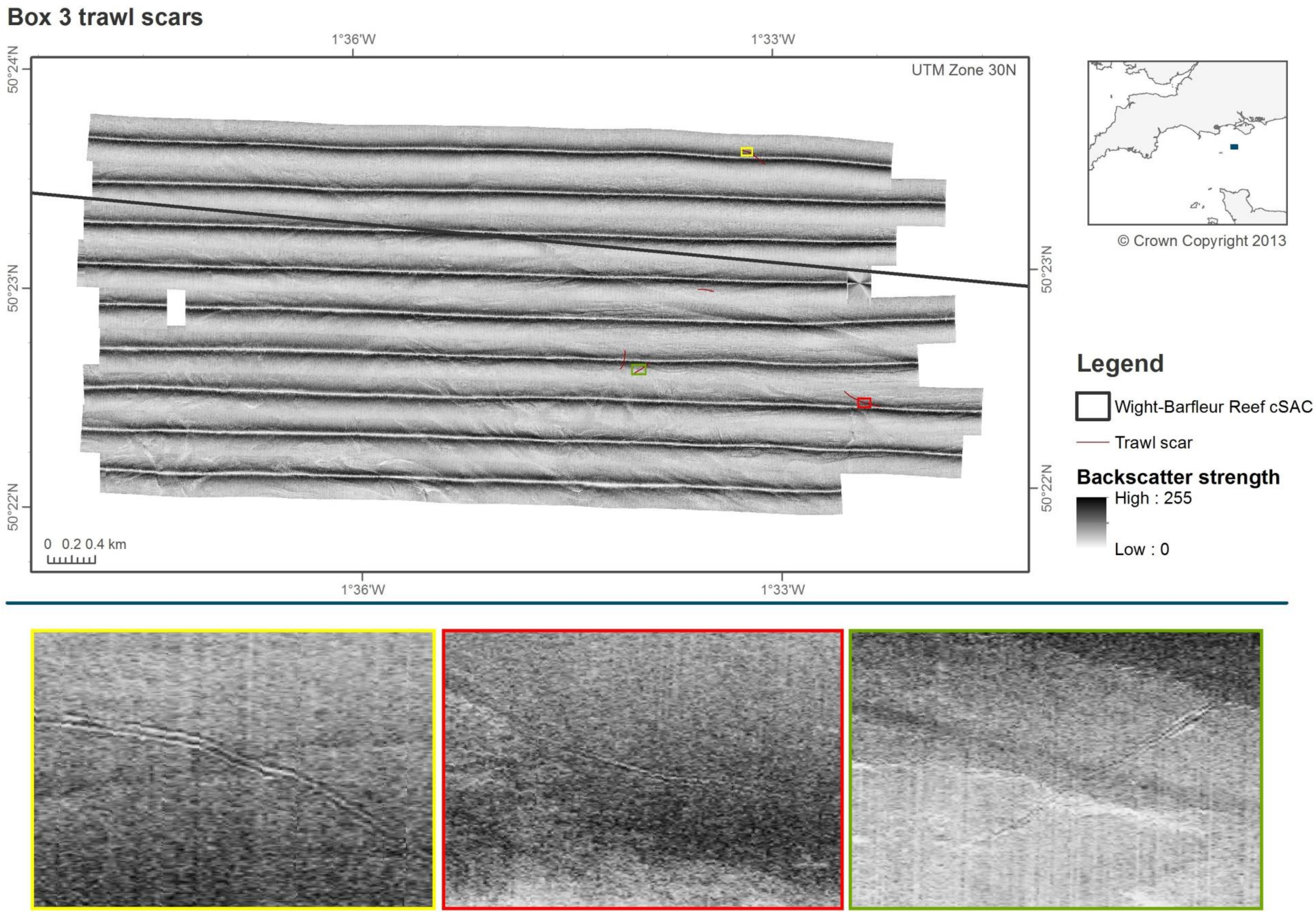

Figure 35. Trawl scars on the seabed at Box 3.

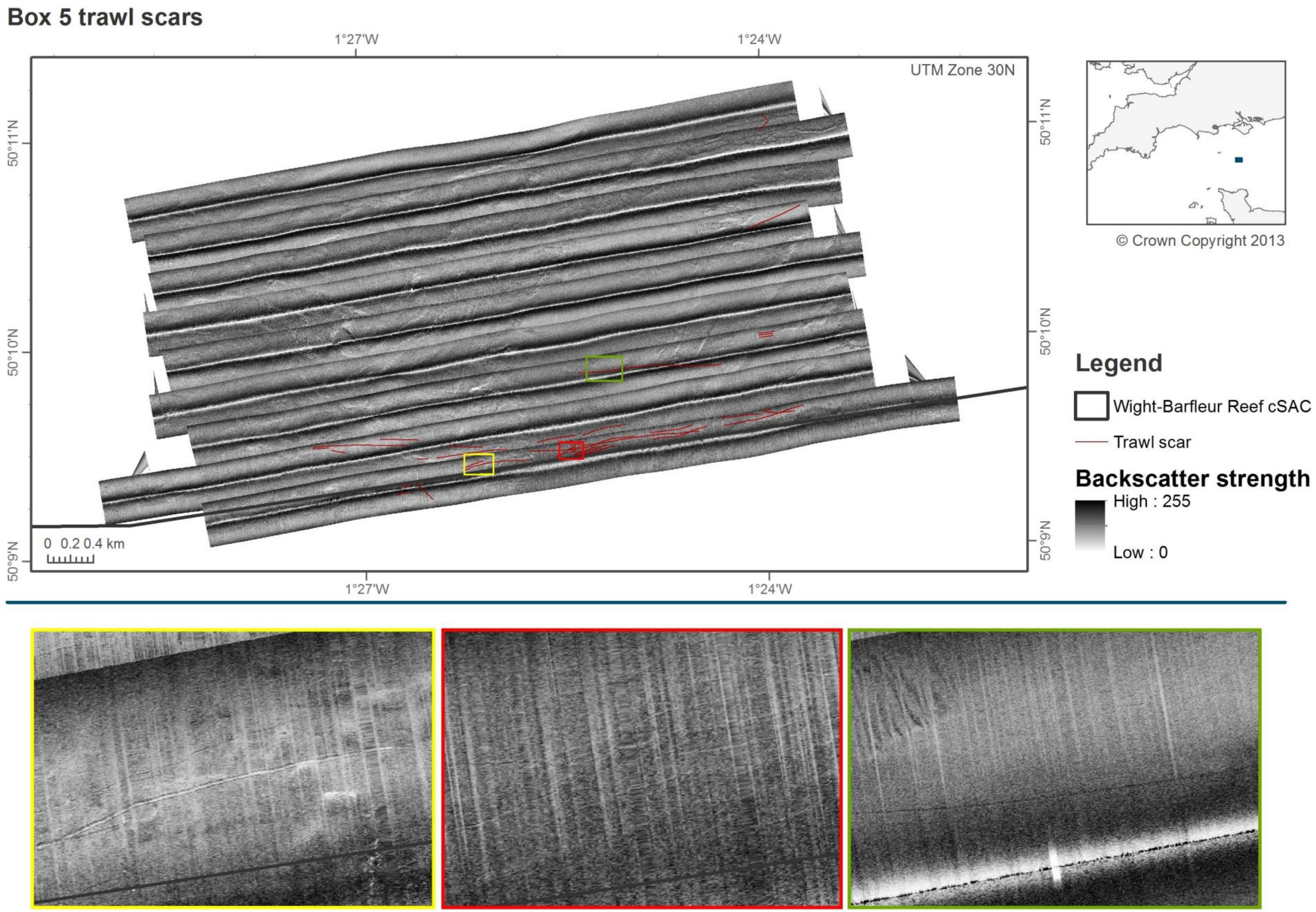

Figure 36. Trawl scars on the seabed at Box 5.

4 Summary

The dedicated 2013 benthic survey of the Wight-Barfleur Reef cSAC was successful in acquiring valuable multibeam, side-scan and ground-truthing data of the seabed. Although full data coverage of the whole cSAC was not possible in the time available, five areas were targeted for intensive survey, with 100% acoustic data coverage of these areas.

Given the predominantly hard nature of the seabed and the lack of differentiation in acoustic signatures between stony reef and coarse sediments, there was little potential to discriminate and map different reef categories based on acoustic features. However, analysis of available data enabled the delineation of Annex I bedrock and boulder reef and confirmed that the concentration of bedrock reef is higher inside the cSAC boundary than outside.

Side-scan sonar returns were not uniform throughout the Wight-Barfleur Reef cSAC, indicating a heterogeneous seabed dominated by bedrock and stony reef, but also with extensive areas of a mosaic of hard and coarse substrates. Smaller, isolated areas of sandy sediments were also observed. Extrapolating the observations made within the intensely surveyed boxes, it is likely that stony reef, or a mosaic of stony reef and coarse sediment, is widespread throughout the cSAC, in between the areas mapped as bedrock reef.

The benthic community observed over the entire survey area was very diverse and variable in its distribution over a small spatial scale, with different variations of the whole assemblage arranged in an irregular mosaic across the entire area. Assemblages inhabiting sedimentary habitats were distinct from those inhabiting harder, more stable substrates, but due to the interspersed nature of these habitats over a small spatial scale and the relatively coarse spatial resolution of the biological data, such habitats and their characteristic assemblages cannot be delineated with precision at the scale of the maps produced in this study. Although there are signs of human activity and physical disturbance still evident on the seabed, no evidence of sustained or permanent damage to the benthic assemblage was observed during this investigation.

References

Blaschke, T. (2010). Object based image analysis for remote sensing. ISPRS Journal of Photogrammetry and Remote Sensing 65, 2-16.

Cameron, A. & Askew, N. (2011). EUSeaMap - Preparatory Action for development and assessment of a European broad-scale seabed habitat map final report. 227pp.

Clarke, K.R. & Gorley, R.N. (2006). PRIMER v6: User Manual/Tutorial. PRIMER-E, Plymouth.

Coggan, R., Diesing, M. & Vanstaen, K. (2009). Mapping Annex I Reefs in the central English Channel: evidence to support the selection of candidate SACs. Scientific Series Technical Report, Cefas Lowestoft, 145: 116pp.

Coggan, R., Barrio Froján, C.R.S., Diesing, M. & Aldridge, J. (2012). Spatial patterns in gravel habitats and communities in the central and eastern English Channel. Estuarine, Coastal and Shelf Science 111: 118-128.

Coggan, R. & Howell, K. (2005). Draft SOP for the collection and analysis of video and still images for ground-truthing an acoustic basemap. Video survey SOP version 5, 10pp.

Collier, J.S., Gupta, S., Potter, G. & Palmer-Felgate, A. (2006). Using bathymetry to identify basin inversion structures on the English Channel shelf. Geology 34, 1001–1004.

Diesing, M., Coggan, R. & Vanstaen, K. (2009). Widespread rocky reef occurrence in the central English Channel and the implications for predictive habitat mapping. Estuarine, Coastal and Shelf Science 83, 647-658.

Hill, M.O. (1973). Diversity and evenness: a unifying notation and its consequences. Ecology 54(2) 427-432.

Holme, N.A. & Wilson, J.B. (1985). Faunas associated with longitudinal furrows and sand ribbons in a tide swept area in the English Channel, Journal of the Marine Biological Association of the United Kingdom Issue 04, November pp 1051-1072.

Hothorn, T., Hornik, K. & Zeileis, A. (2004). Unbiased Recursive Partitioning: A Conditional Inference Framework. Department of Statistics and Mathematics Wirtschaftsuniversität Wien, Research Report Series, Report 8, 16pp.

Long, D. (2006). BGS detailed explanation of seabed sediment modified Folk classification. http://www.searchmesh.net/PDF/BGS%20detailed%20explanation%20of%20seabed%20sediment%20modified%20folk%20classification.pdf

Mason, C. (2011). NMBAQC's best practice guidance: Particle size analysis (PSA) for supporting biological analysis. National Marine Biological AQC Coordinating Committee, 72pp. http://www.nmbaqcs.org/news/nmbaqc/nmbaqc-best-practice-guide-for-particle-size-analysis-is-now-available!.aspx

Owen, K., Newberry, C., Phillips, R., Hearnden, L., Geary, N., Lawler, S., Fletcher, C., Throssell, R., Cloote, J. & Hussey, S. (2013). Analysis of video and stills from Wight-Barfleur Reef 2013. Unicomarine Report CEFVWBFR13 to CEFAS, June 2013.

Reading, H.G. (Ed). (1996). Sedimentary Environments: Processes, Facies and Stratigraphy, Oxford Blackwell Science Ltd.

Stride, A.H. (Ed). (1982). Offshore tidal sands: processes and deposits. London Chapman and Hall Ltd.

Whomersley, P. (2013). Wight Barfleur Reef and Bassurelle Sandbank – SAC Management Survey. Cruise Report, issue date: 04 July 2013, 131pp.

Worsfold, T.M., Hall, D.J. & O'Reilly, M. (2010). Guidelines for processing marine macrobenthic invertebrate samples: a processing requirements protocol version 1 (June 2010). Unicomarine Report NMBAQCMbPRP to the NMBAQC Committee. 33pp.

Appendices

Appendix 1. Infaunal taxon list

List of taxa identified from the two statistically distinct infaunal assemblages represented by more than one grab sample, together with a relative measure of the contribution of each taxon to the similarity within each assemblage.

	Assemblage	
Taxa	**d**	**e**
Sabellaria spinulosa	4.39	
Lumbrineris cingulata	2.03	1.03
Ophiothrix fragilis	2.47	0.4
Nucula nucleus	2.72	
Pisidia longicornis	2.36	0.2
NEMATODA	1.97	0.4
Amphipholis squamata	1.8	0.35
Thelepus setosus	1.38	0.35
Syllis variegata	1.47	0.2
Pyura tessellata	0.98	0.68
Syllis armillaris	1.64	
Sphenia binghami	1.58	
NEMERTEA	0.89	0.68
Laonice bahusiensis	0.38	1.15
ACTINIARIA	1.08	0.4
Aphelochaeta (Type A)	1.17	0.2
Jasmineira elegans	1.17	
Polycarpa pomaria	1.17	
Harmothoe extenuata	1.13	
Pseudopotamilla reniformis	1.08	
Eulalia tripunctata	1.02	
Spirobranchus triqueter	1.02	
Golfingia vulgaris	0.99	
Lepidonotus squamatus	0.84	
Lysidice ninetta	0.82	
Musculus discors	0.82	
Verruca stroemia	0.82	
Polynoe scolopendrina	0.78	
Subadyte pellucida	0.38	0.4
Unciola crenatipalma	0.76	
Eunereis longissima	0.39	0.35
Asclerocheilus intermedius	0.73	
Glycera lapidum (agg)	0.25	0.48
Gibbula tumida	0.52	0.2
Gammaropsis maculata	0.5	0.2
Notoproctus	0.68	
Odontosyllis fulgurans	0.68	
Myrianida	0.66	
Aonides paucibranchiata	0.25	0.4
Leptochiton asellus	0.64	
Nereis zonata	0.6	
Pseudonotomastus southerni		0.6

	Assemblage	
Taxa	**d**	**e**
Sclerocheilus minutus	0.6	
Serpulidae	0.6	
Nematonereis unicornis	0.58	
Sabellidae (juv)	0.56	
Clymenura leiopygos	0.55	
Nicolea venustula	0.34	0.2
Notomastus	0.13	0.4
Alvania semistriata	0.5	
Dipolydora coeca	0.5	
Dendrodoa grossularia	0.48	
Hesiospina similis	0.48	
Eurynome (juv)	0.47	
Anthura gracilis	0.43	
Chlamys varia	0.43	
Syllis gracilis	0.41	
Demonax branchyona	0.4	
Leptocheirus tricristatus		0.4
Phoronis	0.4	
Proceraea	0.4	
Apomatus similis	0.38	
Eumida sanguinea	0.38	
Marphysa sanguinea	0.38	
Pholoe assimilis	0.38	
Cirratulus (juv)	0.35	
Pilumnus hirtellus	0.35	
Rhomboidella prideaux	0.35	
Chaetozone gibber	0.34	
Janira maculosa	0.34	
Timoclea ovata	0.34	
Acanthochitona crinita	0.13	0.2
Exogone verugera	0.13	0.2
Galathea intermedia	0.13	0.2
Gari tellinella	0.13	0.2
Odontosyllis gibba	0.13	0.2
Spirobranchus lamarcki	0.13	0.2
Cyathura carinata	0.31	
Urothoe marina	0.31	
Anapagurus hyndmanni	0.3	
Eulalia mustela	0.3	
Polycirrus	0.3	
Spisula elliptica	0.3	
Dioplosyllis cirrosa		0.28

	Assemblage	
Taxa	**d**	**e**
Leptosynapta inhaerens		0.28
Anomiidae (juv)	0.25	
Apseudes talpa	0.25	
ASCIDIACEA (juv)	0.25	
Callipallene brevirostris	0.25	
Caprella erethizon	0.25	
Chone filicaudata	0.25	
Crepidula fornicata (juv)	0.25	
Eusyllis blomstrandi	0.25	
Glycymeris glycymeris	0.25	
Golfingia elongata	0.25	
Hiatella arctica	0.25	
Limatula subauriculata	0.25	
Malmgrenia arenicolae	0.25	
Petaloproctus	0.25	
Pholoe inornata (sensu Petersen)	0.25	
Styela partita	0.25	
Syllis hyalina	0.25	
Aequipecten opercularis	0.22	
Dipolydora caulleryi	0.22	
Iphimedia eblanae	0.22	
Nephasoma minutum	0.22	
Pterocirrus macroceros	0.22	
Trypanosyllis coeliaca	0.22	
Animoceradocus semiserratus		0.2
Brada		0.2
Diodora graeca		0.2
Eusarsiella zostericola		0.2
Goodallia triangularis		0.2
Mediomastus fragilis		0.2
Ophiuridae (juv)		0.2
Pista cristata		0.2
Scalibregma celticum		0.2
Sphaerodorum gracilis		0.2
Sphaerosyllis bulbosa		0.2
Syllis (Type A)		0.2
Syllis cornuta		0.2
Synaptidae (juv)		0.2
Ampelisca diadema	0.18	
Atylus swammerdamei	0.18	
Demonax torulis	0.18	
Galathea strigosa	0.18	
Heteromysis	0.18	
Leptochiton cancellatus	0.18	
Perkinsiana rubra	0.18	
Sphaerodoropsis distichum (?)	0.18	
Tricolia pullus	0.18	
Tritaeta gibbosa	0.18	

	Assemblage	
Taxa	**d**	**e**
Urothoe elegans	0.18	
Amphilochus manudens	0.13	
Aonides oxycephala	0.13	
Aphroditidae (juv)	0.13	
Arabella iricolor	0.13	
Axionice maculata	0.13	
Balanus crenatus	0.13	
Buccinum undatum (juv)	0.13	
Caprella equilibra	0.13	
Chaetopteridae	0.13	
Cheirocratus intermedius	0.13	
COPEPODA	0.13	
Dorvillea erucaeformis	0.13	
Ebalia tuberosa	0.13	
Ericthonius punctatus	0.13	
Eualus pusiolus	0.13	
Euclymene	0.13	
Eulalia bilineata	0.13	
Exogone dispar	0.13	
Gammaridae (juv)	0.13	
Gattyana amondseni	0.13	
Glycera oxycephala	0.13	
Gnathiidae (juv)	0.13	
Grania	0.13	
Iphimedia perplexa	0.13	
Kellia suborbicularis	0.13	
Laonice sarsi	0.13	
Lumbrineriopsis paradoxa	0.13	
Maera othonis	0.13	
Malacoceros	0.13	
Marphysa bellii	0.13	
Modiolarca tumida	0.13	
Moerella pygmaea	0.13	
Monocorophium sextonae	0.13	
Notocirrus scoticus	0.13	
NUDIBRANCHIA	0.13	
Orbinia sertulata	0.13	
Perrierella audouiniana	0.13	
Pholoe baltica (sensu Petersen)	0.13	
Pseudoprotella phasma	0.13	
Puncturella noachina	0.13	
Semierycina nitida	0.13	
Siphonoecetes kroyeranus	0.13	
Stenopleustes nodifer	0.13	
Syllis garciai (?)	0.13	
Syllis pontxioi	0.13	
Tapes rhomboides (juv)	0.13	
Thelepus cincinnatus	0.13	

	Assemblage	
Taxa	**d**	**e**
Trivia arctica	0.13	
Websterinereis glauca	0.13	
Lagotia viridis		
Pisione remota		

	Assemblage	
Taxa	**d**	**e**
Saccocirrus papillocercus		
Sagitta		

Appendix 2. Epifaunal taxon list

Relative contribution of each taxon to the similarity within the distinct epifaunal assemblages identified from the analysis of data from video and stills. List limited to the taxa contributing to 90% of the similarity within each assemblage and to assemblages represented by more than a single sample. Assemblages ordered left to right by decreasing total number of taxa.

	Assemblage																							
Taxa	**s**	**q**	**r**	**y**	**t**	**e**	**f**	**k**	**n**	**w**	**ac**	**l**	**j**	**o**	**h**	**p**	**c**	**m**	**z**	**d**	**g**	**u**	**aa**	**ad**
Actinopterygii															0.67									
Actinothoe sphyrodeta																								1
Aequipecten opercularis				0.9						1									1					
Alcyonidium diaphanum	0.64		0.55					1																
Alcyonium digitatum		0.79	0.82	0.95	0.92	0.71		1	0.89		0.79	0.5		1	1						1			
Ascidiella										1														
Asterias rubens				0.65																1		0.5		
Axinellidae		0.68	0.64																					
Bispira															1									
Brachyura					0.38																			
Bugula					0.54																			
Calliostoma zizyphinum	0.64	0.84	0.91	0.55	0.62	0.5	0.67	1	1	1		0.75	1	1	1	1					1			
Caryophyllia															1									
Cirripedia	0.73	0.53	1			0.93	0.58					0.75		1	0.67		0.57	1		1				
Cliona celata															0.67									
Corymorpha															0.67									
Corynactis viridis					0.46				0.67	1														
Crossaster papposus		0.63					0.67		0.78		0.64	1						1	0.75		1			
Diazona violacea																			0.5					
Dysidea fragilis	0.73	1	0.73			0.79																		
Ebalia										1			1											
Epizoanthus																						0.5		
Fissurellidae								1																
Flustra foliacea	0.64	0.95	1		0.92	1	0.83	1	0.78		0.93	1	1	1	1	1		1	0.75	1			1	1
Gibbula	0.91	0.84	0.64			0.93	0.75	1				0.75				1	0.71							
Halichondriidae	0.91																							
Hemiasterellidae_Arborescent			0.64																					
Hemimycale columella										1														
Henricia	0.82	0.68	0.91	0.85	0.54	0.79			1	1	1	1	1		0.67			1					1	1
Hyas																			0.5					
Hymedesmiidae	0.91		0.73			1								1	0.67									
Hymedesmiidae_Cushion			0.64																					

	Assemblage																							
Taxa	**s**	**q**	**r**	**y**	**t**	**e**	**f**	**k**	**n**	**w**	**ac**	**l**	**j**	**o**	**h**	**p**	**c**	**m**	**z**	**d**	**g**	**u**	**aa**	**ad**
Hymedesmiidae_Encrusting		1	0.64		0.54											1								
Hymedesmiidae_Globular					0.85																			
Majoidea														1				0.67						
Nemertesia antennina				0.85						1	0.79													1
Ophiocomina nigra																						1		
Ophiothrix fragilis																						1		
Ophiuroidea							0.5										0.57				1			
Pachymatisma johnstonia			0.55	0.65	0.62				0.89		0.71		1	1	1									
Paguridae	0.64	0.79				0.64	0.92	1		1						1	0.57							
Pectinidae	0.91	0.68				0.71	0.42	1	0.89			1				1	0.57	1						
Pentapora foliacea	0.73	0.95	0.64	0.8	0.77	0.64			0.89	1	0.93			1		1				1				1
Polymastia boletiformis						0.64					1				1									1
Polyzoniae	0.73																							
Pomatoceros				0.85						1									1			1		
Porella compressa				0.6																				
Protula tubularia				0.6																		0.75		
Sabellaria spinulosa		1						1	1			1		1	0.67			1			1			
Sabellidae																1								
Sagartia elegans				0.55						1														
Sagartia troglodytes										1														
Sagartiidae	0.73	0.89			0.92	0.86		1	0.89			1		1		1							1	
Serpulidae	1	1	1		0.92	0.93	1	1	1	1		1	1	1		1	1	1		1	1			
Solasteridae													1											
Spongionella pulchella						0.93																		
Stelletta grubii											0.43													
Stelligera stuposa				0.8															0.5					
Terebellidae				0.65																				
Terebratulina										1														
Tethyidae										1	0.43													
Tubularia	0.91	0.68	0.64		0.69	0.71	0.58	1	0.89						0.67			0.67						
U. anemone	0.82	0.79	0.91				0.5	1			0.5	0.75	1	1			0.71	0.67	0.5	1				
U. ascidian_Colonial			0.64					1	0.89				1			1		0.67						
U. ascidian_Solitary	1	1	1	0.9	0.92	1	0.75	1	1		0.86	1	1	1	1	1	0.86	1	1		1			
U. asteroid															1									
U. bryozoan_Encrusting	0.73	1	0.91		0.46		0.58	1	1			1	1	1			1			1				
U. bryozoan_Turf				1											0.67				1		1	1		
U. decapod		0.63	0.73											1		1								
U. echinoderm													1											

	Assemblage																							
Taxa	**s**	**q**	**r**	**y**	**t**	**e**	**f**	**k**	**n**	**w**	**ac**	**l**	**j**	**o**	**h**	**p**	**c**	**m**	**z**	**d**	**g**	**u**	**aa**	**ad**
U. faunal turf	1	0.95	0.91				0.58					0.75	1		0.67		0.57			1	1			
U. gastropod	0.91	1				0.79	0.67	1	1			1		1		1	1	1						
U. hydroid crust										1	0.93												1	
U. hydroid_Erect		1			0.69								1											
U. hydroid_Thecate	0.91	0.89	1		1	1	0.92	1	1				1	1	1	1					1			
U. hydroid_Turf	1		1										1		1			1			1			
U. red algae_encrusting																			0.5					
U. sponge_Arborescent	0.55	0.95	0.82	0.6	0.92				1	1	0.71			1	1	1		1	0.75		1			
U. sponge_Columnar	0.64							1	1			1	1											
U. sponge_Cushion	1	0.84	0.91	0.95	0.38		0.5			1	1		1						0.75				1	1
U. sponge_Encrusting	1	1	1	1	1	1	1	1	1		1	1	1	1	1	1		1	1	1	1	0.75		1
U. sponge_Globular	0.64	1	1		1			1	1			1	1		0.67	1								
U. sponge_Massive			0.82	1	0.62									1	1			1	1					
U. sponge_Papillate									1															
Urticina felina	0.73	0.74		0.55	0.46	0.86	1		0.89		0.43	1						1	1			0.75	1	
Veneroidea						0.64																		
Total no of taxa	97	92	87	69	65	61	50	49	47	47	46	45	43	40	38	36	34	34	34	25	25	23	20	20

Appendix 3. QA reports

The following reports and files which contain the outputs from QA protocols are available on request:

- Quality Control - Stills.xls
- Quality Control - Video.xls
- Wight Barfleur Reef_Video and stills QA sheet.xlsx
- UKAS Report LAB-02_412804_White-Barfleur Reef Sponge and Cobbles_AMENDED.xls
- Wight Barfleur Extension_Video analysis_MAC_QAd.xls

THIS PAGE INTENTIONALLY BLANK

Cefas

JNCC
Joint Nature Conservation Committee

JNCC/Cefas Partnership Report Series. *Offshore seabed survey of Wight-Barfleur Reef SAC*, **No. 24**. Barrio Froján, C., Diesing, M. & Rance, J. September 2021. ISSN 2051-6711